Tectonic and thermal history of the Southern Chotts Basin

Implications on Petroleum Systems in Central Tunisia

J.W.W. Kwakman

Tectonic and Thermal history of the Southern Chotts Basin:
Implications on Petroleum Systems in Central Tunisia

J.W.W. (Jos) Kwakman
(4366492)

Submitted in partial fulfillment of the requirements for
the degree Master of Science in Petroleum Engineering & Geosciences

Department of Applied Geology
Faculty of Civil Engineering & Geosciences
Delft University of Technology

November 19, 2020

COVER TITLE:
A brief look into the subsurface of the Southern Chotts Basin

COVER DESIGN:
Paul van Sommeren

THESIS COMMITTEE:
Prof. Dr. G. Bertotti
Dr. P.B.R. Bruna
Dr. A. Barnhoorn
Prof. Dr. A.W. Martinius

LOCATION:
Faculty of Civil Engineering & Geosciences
Stevinweg 1, 2628 CN Delft
The Netherlands

DATE:
November 19, 2020

ABSTRACT

The primary reservoirs present in the Southern Chotts Basin, Central Tunisia, are located within Triassic, Permian and Ordovician units. They are mainly sourced by the Silurian – Lower Devonian Fegaguira formation and its Hot Shale member. Late Paleozoic exhumation has eroded part of the Palaeozoic package, removing the Early Devonian – Carboniferous and most of the Permian deposits in the Southern Chotts Basin. This resulted in a diachronous unconformity in the present-day stratigraphy and represents significant uncertainties.

This study presents a reconstruction of the tectonic and thermal history of the Southern Chotts Basin and the subsequent impact on source rock thermal maturation, with an emphasis on the Hercynian exhumation. Implications on the petroleum systems in the basin are evaluated by means of a migration study.

Investigation of adjacent analogue basins allows estimation of the amount of initially deposited sediment in the Early Devonian – Permian. Calibration with vitrinite reflectance data minimizes exhumation uncertainties in the basin history and indicates ca. 2300 m sediment eroded during the Hercynian phase.

Subsidence analysis shows similar subsidence patterns throughout the area of interest since the Mesozoic. This argued to use a single set of high and low case initial deposition estimates, calibrated with vitrinite reflectance, in source rock maturation modelling.

Source rock maturation modelling in the kitchen area indicates hydrocarbon generation occurs in two phases separated by a phase of stable maturity during Hercynian exhumation. Maturation in the kitchen area is found to currently be in the condensate – wet gas zone.

Migration modelling shows that Paleozoic generation in the northern and northeastern portion of the basin primarily sourced the present-day hydrocarbon discoveries. High capillary entry pressures in overlying Fegaguira shales forced hydrocarbons generated in the Hot Shale member to migrate downward into porous Ordovician units. Subsequently, hydrocarbons laterally migrate up-dip into local traps, where they remain trapped wherever the overlying source rock is preserved during Hercynian exhumation. The Ordovician units acts as a reservoir, and as a carrier bed to source present-day accumulation in the Triassic TAGI unit.

A newly identified petroleum system primarily hosts accumulations in lower shoreface Ordovician El Atchane deposits, overlain by the Fegaguira and Hot Shales. Simulated hydrocarbon accumulations and projection of shoreface deposits throughout the area of interest mark a sweet spot area with significant reservoir potential in structural traps. Recommendations are given to further investigate the potential of this system.

Keywords: Southern Chotts Basin, source rock maturation, tectonic history, Fegaguira, migration modelling

CONTENTS

Appendix

PREFACE

This thesis marks the end of my research conducted to finalize a Master of Science degree in Applied Earth Sciences. Throughout the year it took me to conduct this thesis I realised academia is a different beast entirely. Conducting thesis research is solitary. Despite this, I had a team of individuals behind me who supported me and wanted me to succeed.

Firstly, I would like express my gratitude to my thesis committee; Giovanni Bertotti, Pierre-Olivier Bruna, Auke Barnhoorn and Allard Martinius. Giovanni and Pierre-Olivier mentored me from the start of the project and helped shape and reshape the project throughout its duration. I would like to thank Pierre especially, for his immense amount of encouragement and motivation. Pierre was always available for discussions and has put in many more hours than I dared ask of him. Without you Pierre, I would never have presented my research on a conference and made it what it is today. Additionally, Pierre is an excellent barista who serves great coffee if you visit him. Giovanni, thank you for providing me with critical insights and pushing me to improve on the reasoning in my thesis. You always knew how to point out the missing links and helped me shape the final product. Auke and Allard, my thanks to you for providing invaluable and constructive feedback during the final months of the project.

Secondly, I would like to acknowledge Mazarine Energy for their contribution to this project within the North African Research Group. Special credit must be awarded to Salma Ben Amor for supporting our research at TU Delft. Thank you for helping realize this project and providing us with the data used throughout our research.

Thirdly, my thanks go out to my fellow students in the MSc and PhD office. Special thanks here to my fellow graduate and friend Ruaridh Smith, with whom I had the opportunity to work closely throughout the project. Not only did we discuss our thesis related troubles and successes during our standardized coffee breaks, we also spoke often about what was going on in our personal life. Thank you and the best of luck with your PhD.

Lastly, I would like to express special gratitude to Paul van Sommeren for his creative support and wonderful cover design.

Since this document also marks the end of my journey as a student at the Delft University of Technology, I would also like to thank some people who've helped shape me to the person I am today. They have made my time in Delft unforgettable and I would like to thank them in my native language.

Dit is het dan, het is klaar. Op het moment dat je dit leest heb ik aan het langste eind getrokken. Ik heb in vreugde een fles champagne geopend, de inhoud in single-phase flow door mijn slokdarm naar binnen laten glijden, en ik mag mij officieel een Delftse ingenieur noemen. Je zou hier natuurlijk een mass balance vergelijking voor op kunnen stellen, maar dat zou niet geheel aansluiten bij het onderwerp van mijn thesis.

Mijn tijd in Delft was een relatief korte ervaring van zo'n 6.237 ± 0.0027 jaar. De eerste aantal jaren zijn het makkelijkst; je komt aan als onwetende eerste jaars in een nieuwe stad en de wereld ligt aan je voeten. Je ontmoet tal van mensen die net zo enthousiast zijn als jij en op zoek zijn naar hun plekje in het mooie Delft. Met velen van hen raak je bevriend

en praat je tijdens de koffiepauzes of met een biertje in de hand over hoe het gaat met de studie, je huis, je ouders, of wat dan ook maar ter sprake komt.

Door de jaren heen leer je hen steeds beter kennen en sommigen van hen worden je goede vrienden. Mensen waarmee je kan lachen, waar je samen mee op avontuur gaat, die je helpen jezelf te ontdekken, waar je tal van hilarische herinneringen mee hebt, die je gelukkig maken. Maar ook mensen waar je op terug kan vallen als het even tegen zit, die je een hart onder de riem steken als je door de bomen het bos niet meer ziet, die je even op andere gedachten brengen als je er door heen zit, die je weten te motiveren als je dat even nodig hebt.

Dit laatste jaar heb ik niet als eenvoudig ervaren en ik heb geleerd dat de academische wereld toch echt andere koek is. Bijkomend aspect is dat er zich een mondiale pandemie voordeed, waardoor sociaal contact geminderd werd en gemaakte plannen van de tafel waren. Stenen hakken in Tunesië zat er dus niet in. Meermaals heeft het tegen gezet, maar nog vaker heb ik daar oplossingen voor weten te vinden met steun van de gemaakte vrienden hier in Delft. Zij hebben gezorgd voor een studententijd om nooit te vergeten. Graag zou ik hen hier mijn eeuwige dank voor toekennen:

De mannen uit Vesc, met wie ik vele uren in de studie banken heb gezeten, maar nog vele uren meer lol mee heb gehad. De heren van de SBLMG, die mijn gedachten met vele avonden scheppen hebben kunnen verzetten. De lieve jongens en meiden van de OD, waarbij ik me geen fijner thuis had kunnen bedenken. De mannen van de NoCo, waarmee ik ten volste van het studenten leven heb genoten. De heren van Projectiel, die mijn studententijd de kick-start gegeven hebben die het nodig had.

Aflsuitend wil ik graag mijn dank uitspreken voor mijn lieve vriendin Renske. We leerden elkaar kennen als twee van die onwetende eerste jaars, wat voortvloeide tot een hechte vriendschap. Jij was één van die mensen waarmee je kon lachen, waarmee je avonturen beleefde, en waar je op kon rekenen als het even tegen zat. Inmiddels sta je al bijna 4 jaar door dik en dun voor me klaar en heeft jouw enthousiasme me meermaals uit die welbekende sleur getrokken. Bedankt voor alle vrolijkheid die je in mijn leven brengt, de activiteiten die je organiseert om mij op andere gedachten te brengen, de mooie reizen die je met mij wilt maken, en de liefde die je me geeft. Zonder jou was dit niet gelukt!

Veel dank ook naar mijn oudere broer Koen, die evenals ik een geweldige tijd hier in Delft heeft beleefd. Als de Benjamin in huis bewandel je veelal een pad dat jij als oudere broer hebt vrijgemaakt. Jouw keuzes waren vaak een inspiratie voor wat er mogelijk was. Dit heeft mij de afgelopen 25 jaar alle vrijheid gegeven waardoor ik heb kunnen gaan en staan waar ik wilde.

Dan als laatst, maar zeker het belangrijkst, mijn lieve ouders: Wim en Rina Kwakman. Van kleins af aan hebben jullie mij onvoorwaardelijk gesteund in zo'n beetje alles wat ik maar wilde doen. De tal van ouderlijke lessen door de jaren, waaronder 'Draag elke dag een schone onderboek', zullen me altijd bij blijven. Misschien is 'tevreden zijn met wat je hebt' wel de belangrijkste les die jullie mij leerden. Zo wisten jullie meermaals mijn problemen te relativeren door een andere blik op de situatie te werpen. Dankzij jullie vertrouwen, steun en liefde kijk ik met een voldaan gevoel terug op mijn studententijd. Ik hoop dat ik jullie hier ooit genoeg voor kan bedanken. Om alvast te beginnen: Bedankt!

Jos Kwakman
Rotterdam, November 2020

1 INTRODUCTION

The Southern Chotts Basin, located in Central Tunisia (figure 1.1), is a proven prolific petroleum province since the early 1980s. Gas and condensate discoveries in the Triassic and Ordovician units are sourced by Silurian – Early Devonian Fegaguira formation (Mejri et al., 2006; Soua, 2014a). The basin-fill primarily consists of Paleozoic and Mesozoic packages which are separated by an unconformity as a result of exhumation and erosion (Gharsalli and Bédir, 2020; Raulin et al., 2011; Soua, 2014b). Seismic data and interpretation suggests that this unconformity represents a major time gap as large as Early Devonian to Triassic in the Southern Chotts Basin (figure 2.2). Associated uncertainties in timing and amount of eroded sediment manifest in the tectonic history of the basin.

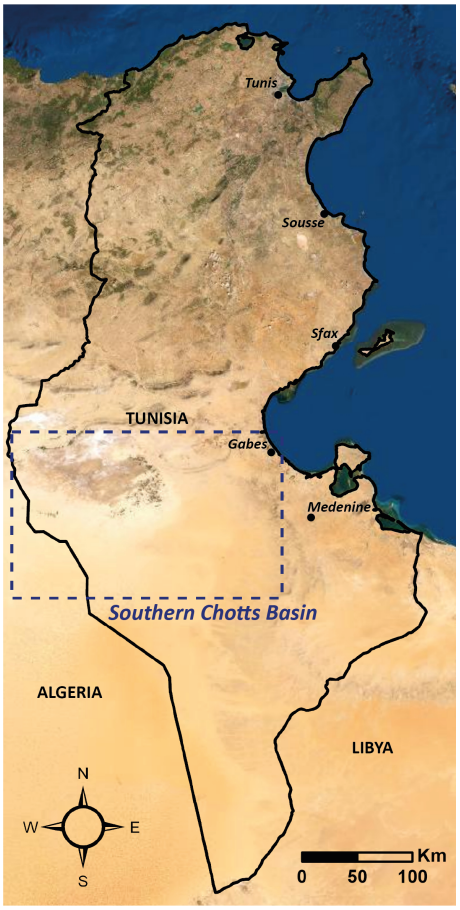

Figure 1.1: Location of the Southern Chotts Basin, Central Tunisia.

Hydrocarbon generates by thermal decomposition of organic matter, which is primarily controlled by temperature and time. It is therefore that the basins tectonic and thermal evolution significantly controls the petroleum source generation history (Allen and Allen, 2013; Underdown and Redfern, 2008). Subsequently, the basin evolution influences the distribution of matured source rock and the location of the hydrocarbon kitchen. It also affects hydrocarbon migration, trapping and preservation, and therefore has large implications on the petroleum systems in the Southern Chotts Basin (Magoon and Dow, 1994).

This thesis presents a reconstruction of the tectonic and thermal history of the Southern Chotts Basin and the subsequent impact on source rock thermal maturation, with an emphasis on the Late Paleozoic exhumation. The implications on the basins petroleum systems are evaluated by means of a migration study. This is realized through the following research questions:

1. What is the tectonic and thermal history of the area of interest?
2. How do exhumation phases affect the source rock maturation history?
3. How does hydrocarbon migrate from source to present-day accumulations?
4. What are the implications of the proposed basin history on the petroleum systems within the basin?
5. What could be potential exploration targets within the area of interest?

2 GEOLOGICAL SETTING

The area of interest is located in the Southern Chotts Basin on the Saharan platform in Central Tunisia (figure 2.1). The basin is bounded to the north by the Atlasic domain, to the west by the neighbouring Jeffara Basin, and to the south by the Telemzane Arch (figure 2.1). Cretaceous – Quaternary deposits predominantly outcrop in the Southern Chotts Basin. The adjacent Jeffara Basin hosts the only North African outcropping Marine Permian deposits in the Tebaga de Medenine (Raulin et al., 2011).

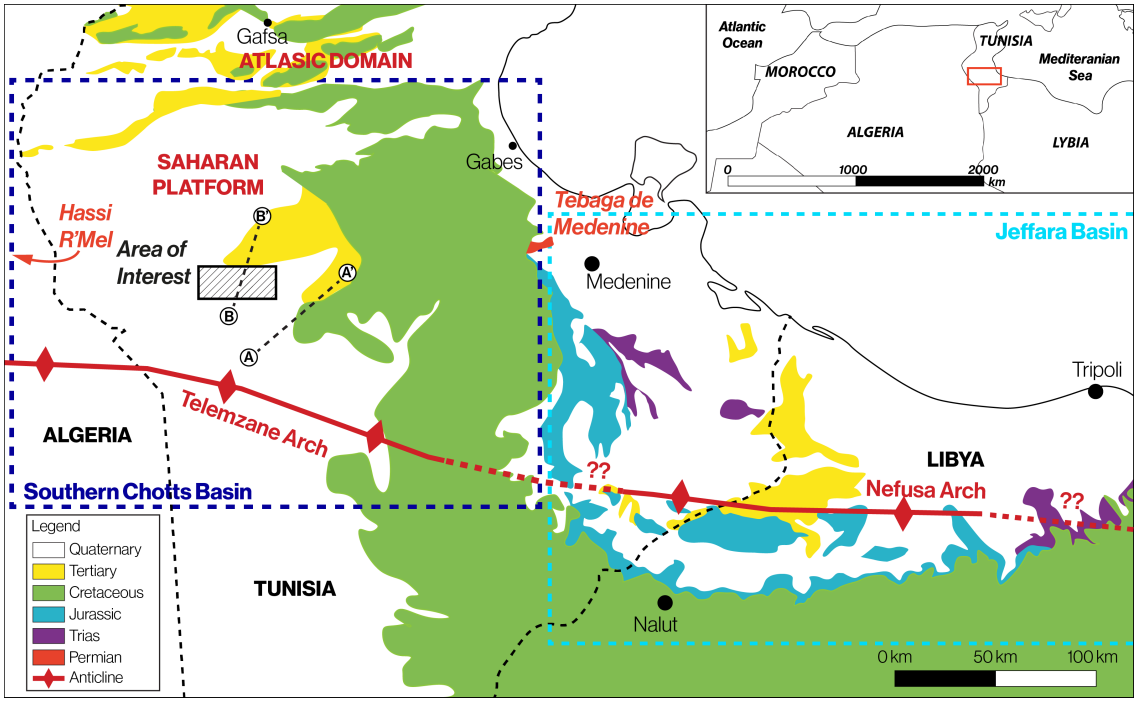

Figure 2.1: Schematic depiction of the geological setting of Central Tunisia and its surroundings. Cretaceous – Quaternary deposits outcropping at the surface cover the Southern Chotts Basin. The Atlasic domain and the Telemzane arch form the boundaries of the Southern Chotts Basin in the north and south respectively. The area of interest is indicated on the map, north of the Telemzane Arch. Location of the seismic transects (figures 2.2 & 4.4) are marked. Amended from (Bruna et al., 2019a)

The Southern Chotts Basin consists of a Precambrian metamorphic basement, covered by Paleozoic (Cambrian – Permian) formations unconformably overlain by Mesozoic (Triassic – Cretaceous) formations. This sedimentary series is overlain by a thin package of Tertiary deposits (figure 2.2) (Bishop, 1975; Galeazzi et al., 2010).

There is a vast difference in terms of geometry and structure of the Mesozoic and Paleozoic formations (figure 2.2). The Palaeozoic formations experienced deformation and truncation likely relates to Late Paleozoic exhumation creating a major unconformity. This unconformity records a gap as large as Early Devonian to Triassic and truncates for-

mations as old as the Ordovician (figure 2.2). The Devonian, Carboniferous and (part of) the Permian are missing in most of the Southern Chotts Basin (Frizon de Lamotte et al., 2013; Mejri et al., 2006). The overlying Mesozoic deposits have experienced less deformation, show gentle large scale folding and an unconformity in the Cretaceous (Bruna et al., 2019b).

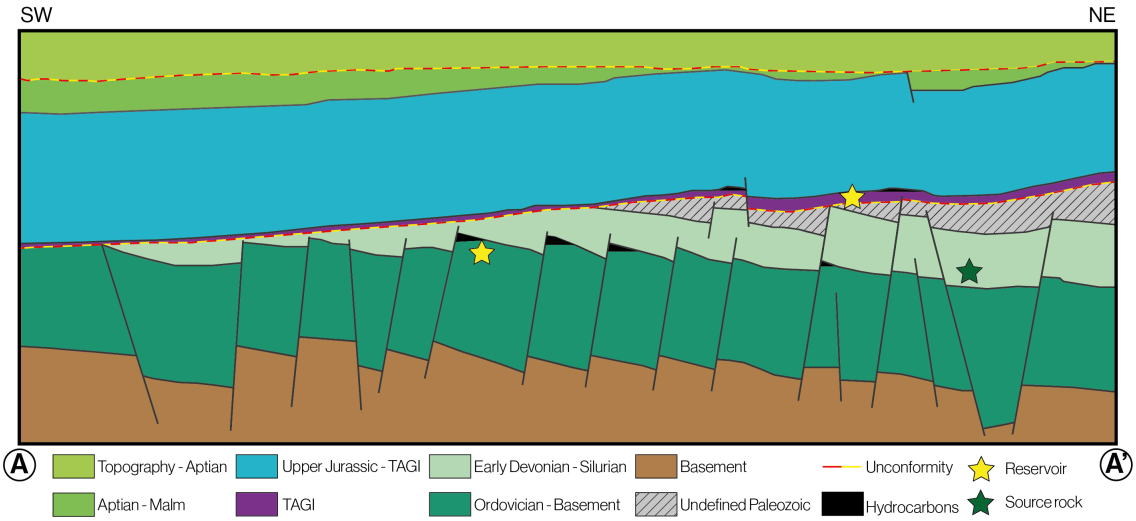

Figure 2.2: Schematic depiction of the present-day structure of the Southern Chotts Basin based on seismic imaging (location in figure 2.1). Important reservoirs are hosted in the Triassic TAGI- and Ordovician Hamra, El Atchane and Jeffara units. The most prominent source rock are the Silurian – Early Devonian Fegaguira and its Hot Shale Member.

2.1 GEOLOGICAL HISTORY

During the Infracambrian (Neoproterozoic – Early Cambrian), North Africa experienced major extensional- and strike-slip movements, creating arches and basins. This time also marks the set-up of the Telemzane Arch (figure 2.1), a major E – W trending structural element that later influenced the deposition location of Early Ordovician formations. Marine transgression dominated the Early Ordovician North Africa which resulted in mostly continental and shallow marine siliciclastics north of the Telemzane Arch, i. e. *El Atchane*, *Hamra*, and *Azel* formations (Bruna et al., 2019a; Lüning, 2005).

In the Late Ordovician, the North African margin of Gondwana drifted over the South Pole causing extensive glaciation across North Africa and a global lowstand of sea level (Guiraud et al., 2005; Jabir et al., 2020). This glacial event resulted in a gentle but widely registered unconformity which locally eroded underlying deposits, e. g. Ordovician *Azel* shales, creating accommodation space for deposition of the Ordovician *Jeffara* unit (Guiraud et al., 2005; Jabir et al., 2020; Mejri et al., 2006; Soua, 2014b). Subsequent deglaciation during the Silurian causes major transgression and flooding of the North African Platform resulting in deposition of organic rich, deep marine *Fegaguira* shales and its Hot Shale member (*"Hot Shales"*) in topographic lows (Guiraud et al., 2005; Lüning et al., 2000; Soua, 2014b).

During the Devonian and Carboniferous, the basins adjacent to the Telemzane Arch, experienced significant extension (Frizon de Lamotte et al., 2013; Galeazzi et al., 2010). South of the arch this led to deposition of a preserved Devonian – Carboniferous package containing mostly shallow marine sediments in the Berkine – Ghadames basins (Galeazzi

et al., 2010; Soua, 2014a; Underdown and Redfern, 2008). North of the arch, Frizon de Lamotte et al. (2013) show unconformable Carboniferous – Silurian contacts in the Jeffara and Hassi R'Mel areas, on the eastern and western continuations of the Telemzane Arch respectively (Galeazzi et al., 2010). This indicates a Late Devonian – Early Carboniferous exhumation phase, removing the Devonian package and making the Telemzane Arch a regional high since the Late Devonian. Subsequent deposition of the Carboniferous marine sediments occured in post-rift sag basins flanking the north and south of the arch, resulting in this unconformity (Frizon de Lamotte et al., 2013).

The Southern Chotts Basin shows Ordovician – Early Devonian units unconformably overlain by Permian to Triassic formations, implying a major time gap as large as Ordovician – Triassic (figure 2.2). Two regional unconformities can be distinguished dating to the Late Carboniferous and the Late Permian – Early Triassic (Bruna et al., 2019b; Frizon de Lamotte et al., 2013). These are generally stacked together and are likely related to the long-lived "Hercynian" tectonic episode caused by closure of the Paleo-Thethys Oceans. (Frizon de Lamotte et al., 2013; Galeazzi et al., 2010; Guiraud et al., 2005; Mejri et al., 2006). In the area of interest the complete Early Devonian – Permian package is missing, leaving the local nature of the Hercynian phase(s) to remain uncertain.

Pangea started breaking up during the Late Permian leading to the opening of a new Tethys Ocean and associated rift stages till the Early – Mid Triassic (Bouaziz et al., 2002; Frizon de Lamotte et al., 2013). As rifting progressed, Triassic syn-rift continental sequences unconformably blanketed Permian and older formations, which transgressed southwards across the Hercynian unconformity (Boote et al., 1998; Bouaziz et al., 2002; Guiraud et al., 2005). Seismics show this sequence to be poorly faulted and poorly deformed within the Southern Chotts Basin. The Trias Argilo-Gréseux Inferieur member (*TAGI*) of this sequence forms important reservoirs in Southern Tunisia and consists of fluvial sands (Boote et al., 1998; Galeazzi et al., 2010; Soua, 2014b).

The Late Triassic – Early Cretaceous marks a period of persistent extension in Tunisia, where normal E – W trending normal faults formed the Chotts Basin. Tunisia transformed to an epicontinental domain, hosting a vast subsiding sabkha during the Late Triassic – Lower Jurassic, resulting in deposition of evaporites, silts, clays and shallow marine sabkha carbonates (Bouaziz et al., 2002; Galeazzi et al., 2010; Guiraud et al., 2005). Evaporites from this sequence form a caprock for Triassic and Paleozoic reservoirs throughout the Saharan Platform (Galeazzi et al., 2010; Lüning, 2005). Further carbonate syn-rift deposition dominated the Chotts Basin during the Middle Jurassic and Upper Jurassic (Bouaziz et al., 2002).

New interpretation by Smith (2020) offers a different perspective on the tectonics during the Permian – Jurassic. Smith (2020) mentions a Late Hercynian shortening phase occuring between the Late Permian and Early Jurassic is observed in the Tebaga de Medenine (figure 2.1). This phase is characterised at the scale of hunderds of meters of E – W striking folds in which Middle – Late Triassic and Early Jurassic units deposited.

The Jurassic – Cretaceous transition marks the start of a sequence of alternating compression and extension in the Southern Chotts Basin and its surroundings, generally grouped together as the "Austrian" unconformity (Bodin et al., 2010; Bouaziz et al., 2002; Bruna et al., 2019a). In the Southern Chotts Basin this manifested in an unconformity where the Aptian overlies the Upper Jurassic (figure 2.2). This period is sealed by Late Cretaceous carbonates resulting from marine transgression during the Albian (Galeazzi et al., 2010).

Towards the end of the Cretaceous, Africa and Eurasia start colliding, marking the early stages of the the "Alpine" cycle, and closing the remnants of the Tethys oceanic domain (Bouaziz et al., 2002; Galeazzi et al., 2010; Guiraud et al., 2005). According to Mejri et al. (2006), the Southern Chotts Basin was likely emerged during the Paleocene – Miocene preventing deposition. Well data in the area of interest shows Pliocene deposits overlying Late Cretaceous formations, representing a major hiatus.

2.2 PETROLEUM SYSTEM SETTING

Petroleum systems comprise of a body of (previously) matured source rock and includes all essential elements and processes required to accumulate and accommodate hydrocarbons (Magoon and Dow, 1994). The essential elements of a petroleum system include:

1. Organic rich source rock which is sufficiently heated such that it expels petroleum
2. Porous and permeable reservoir rock allowing fluid flow
3. Impermeable cap rock that prevents upward migration of petroleum
4. Sufficient time for migration

These 4 elements should occur such that petroleum is trapped and accumulated. The timing of trap formation, petroleum generation, migration and accumulation is essential and must occur in a favorable sequence. Trapped petroleum accumulations must be preserved from e. g. breaching, bio-degradation, and/or thermal degradation, in order to be exploited. (Magoon and Dow, 1994; Selley and Sonnenberg, 2015).

The Southern Chotts Basin petroleum blocks contain 2 proven petroleum systems, namely the Ordovician and Triassic petroleum systems (figure 2.2). The primary source rock for both the Ordovician and Triassic petroleum systems are Silurian – Early Devonian Fegaguira shales and its lower Hot Shale member ("Hot Shales") (Bruna et al., 2019b; Derguini et al., 2005; Mejri et al., 2006). In the area of interest, the upper part of the Fegaguira Formation contains thick packages of mostly interbedded shales and siltstones. The Hot Shale member deposited in deep marine environment under anoxic conditions and has the most promising source rock properties (Derguini et al., 2005). Well data in the Southern Chotts Basin indicates that these source rocks contain planktonic type II kerogen and have up to 16.6% total organic content resulting in significant generation potential (Derguini et al., 2005; Mohamed et al., 2014; Soua, 2014b). The Fegaguira Formation is regularly penetrated in wells throughout the area of interest, with Hot Shale thicknesses reported between 15 – 108 m, and is buried deeper in the northern section of the area of interest (Derguini et al., 2005; Soua, 2014b).

2.2.1 *Ordovician Petroleum Systems*

The Hamra, El Atchane and Jeffara units comprise the most important Ordovician reservoir rocks, which are reworked by erosion in the Southern Chotts Basins. These reservoir rocks are overlain and sealed by impermeable Azel and Fegaguira shales. These cap rocks are eroded in areas of the Southern Chotts Basin where Triassic volcanics, shales and evaporites (TAGD) now function as the seal. Hydrocarbon accumulates in the Ordovician reservoirs in both structural and stratigraphic traps, where they are prevented from

upward migration by the cap rocks. The structural traps comprise i) low amplitude anticlines, ii) normal fault associated anticlines, and iii) tilted fault blocks. The stratigraphic traps relate to pinch outs beneath unconformities which are overlain by impermeable deposits. (Bruna et al., 2019b; Derguini et al., 2005; Mejri et al., 2006)

The Ordovician El Atchane and Hamra formations are deposited in a NE prograding shallow marine siliciclastic ramp striking NW – SE. The El Atchane Formation consists of clean fine to medium grained meter thick beds of sandstones deposited in a lower shoreface environment (Derguini et al., 2005; Gharsalli and Bédir, 2020). These beds are commonly stacked together into thick sandstone packages containing an average porosity of ca. 8% and permeability of ca. 14 mD. Cementation is mostly related to dolomite and clay cements. The lowermost shoreface facies of the El Atchane Formation offer poorer reservoir characteristics with average porosity of ca. 4% and permeabily of ca. 1 mD. These deposits are well cemented with quartzite cement.

The overlying Hamra Formation, deposited on the upper shore face, contains meter thick beds of clean, highly cemented quarzarenite (Derguini et al., 2005; Gharsalli and Bédir, 2020). The Hamra Formation is believed to be heavily fractured in the vicinity of regional faults (Derguini et al., 2005; Gharsalli and Bédir, 2020). These naturally occurring fractures result in productive reservoirs with fair porosity of ca. 9% but low permeability (1 mD) by compensating the low matrix porosity and permeability (Derguini et al., 2005; Galeazzi et al., 2010; Gharsalli and Bédir, 2020).

The Ordovician Jeffara Formation covers partially eroded underlying Hamra quartzarenite, as a result of the Late Ordovician glacial event, and consists of sub-glacial, glaciomarine and deltaic deposits. The reservoir potential lies in sandstone beds stacked into laterally extensive sheet-like packages. The Jeffara Formation is the equivalent of the Memouniat Formation and Unit IV in the Kufra and Illizi basins respectively (Soua, 2014b). These units host major hydrocarbon reservoirs in Algeria and Libya, and therefore could offer good reservoir potential (Lüning, 2005).

2.2.2 *Triassic Petroleum System*

The fluvial sands found in the TAGI unit are the main reservoir in the Triassic interval. Local tectonics and development of volcanic paleo-highs controlled channel orientation, forcing fluvial channels to deposit stacked sandbodies in N – NE direction (Derguini et al., 2005). The TAGI fluvial nature manifests in rapid lateral reservoir thickness and facies changes. The best reservoir potential is found in the stacked TAGI sands, where porosity ranges from 2 – 24%, permeability is generally less than 100 mD and the reservoir thickness varies between 50 – 100 m (Derguini et al., 2005; Mejri et al., 2006). The Net-to-Gross of these fluvial deposits ranges between 20 – 50% in the west and east respectively. An extensive regional seal is provided by Triassic shales overlain by Triassic evaporites. Structural and stratigraphic traps (e. g. pinch outs and lateral lithofacies changes) accumulate hydrocarbon in the TAGI unit, which is prevented from upward migration by the seal (Bruna et al., 2019b; Derguini et al., 2005; Mejri et al., 2006)

3 CONCEPTS & METHODOLOGY

This study analyses tectonic and thermal history of the Southern Chotts basin, calibrates them with maturation data, and models source rock thermal maturation and transformation. The goal is to get insight in e. g. source rock maturation, petroleum generation, migration, reservoir charging and the timing of these processes (figure 3.1) (Bora and Dubey, 2015; Underdown, 2006). Subsequent 2D migration studies on selected transects, capturing the potential kitchen area and 3D structure, identifies migration pathways that sourced present-day hydrocarbon accumulations in the Southern Chotts Basin.

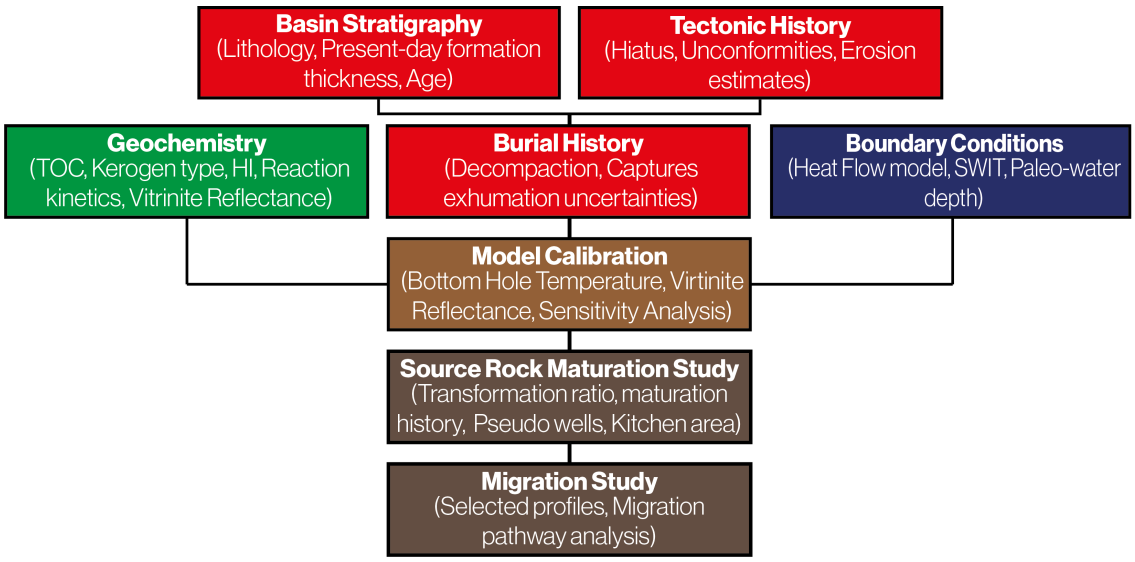

Figure 3.1: Basin modelling workflow including primary input parameters and basin modelling objectives. Amended based on Bora and Dubey (2015)

3.1 SOURCE ROCK GEOCHEMISTRY

3.1.1 *Model Input*

Petroleum is sourced from organic-rich rocks, i. e. source rocks, as a result of exposure to increased temperatures over extended periods of time. Characterising the source rock in terms of *Total Organic Carbon* (TOC) and *kerogen* type allows modelling of its generation potential (Allen and Allen, 2013).

TOC is a measure of organic content contained within a rock, expressed as a ratio between the rocks carbon and total mass. Kerogen generally makes up the majority of the TOC (Allen and Allen, 2013; Hantschel and Kauerauf, 2009). As kerogen thermally decomposes, petroleum expels from the source rock, decreasing the present-day TOC. Initial TOC may therefore be significantly higher than the present-day TOC measured in matured source rock (Peters et al., 2006; Underdown, 2006).

Kerogen types are classified based on their composition and depositional environment (Hantschel and Kauerauf, 2009). Petroleum kinetics models describe kerogen thermal decomposition within a specific source rock and should only be used if the analogue is appropriate (Bora and Dubey, 2015; Peters et al., 2006).

Source rock maturation and generation potential are modelled using geochemical data from production and exploration wells (location in figure 3.5). The maximum TOC, measured in matured source rock, serves as input for source rock average initial TOC used in maturation modelling. Kerogen type was identified in exploration work on the area of interest by Derguini et al. (2005). In absence of source rock kerogen kinetic data in the Southern Chotts Basin, this thesis will use a laboratory calibrated kinetic model from an analogue source rock.

3.1.2 *Calibration Parameters*

To further constrain the timing of source rock maturation, the proposed burial and heat flow models can be calibrated with present-day and paleo-temperature data from exploration and production wells, e. g. corrected Bottom Hole Temperature (BHT) and Vitrinite Reflectance (VR) (Allen and Allen, 2013; Underdown et al., 2007).

Measured BHT are typically lower than 'true' formation temperatures due to cooling associated with drilling mud and have to be corrected. The Horner correction compensates this by means of *Time Since Last Circulation* (TSLC) and is the most widely used method in basin modelling (Harris and Peters, 2012; Welte et al., 1997).

VR is a non-reversible maximum paleo-thermometer that initially increases with temperature; i. e. VR does not decrease with decreasing temperatures, and once a sample reaches a certain temperature it will not increase until that temperature is exceeded (figure 3.2, **left**). In addition, it is predictable with temperature which makes it useful for burial history and paleo-heat flow model calibration (Allen and Allen, 2013; Sweeney and Burnham, 1990).

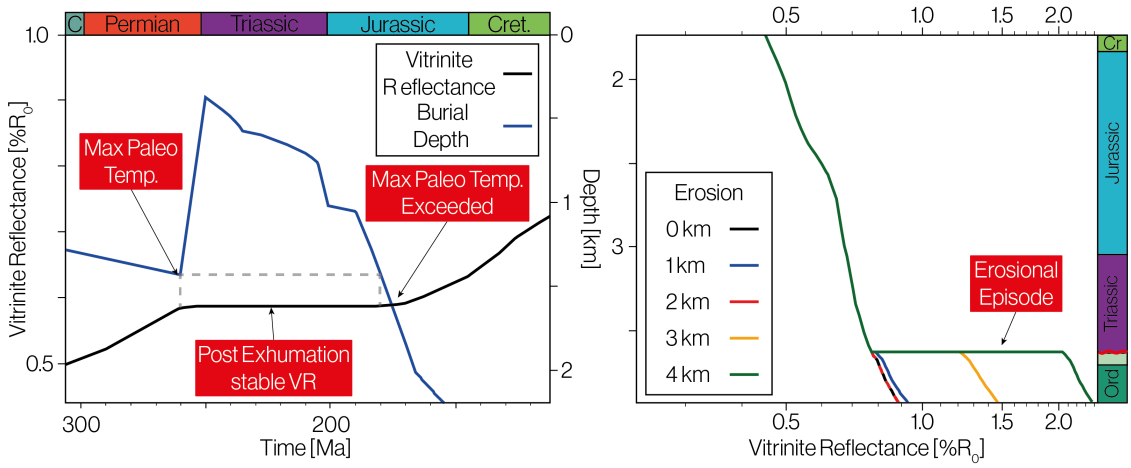

Figure 3.2: **Left:** Conceptual evolution of VR with increasing burial, where VR maturation stops after exhumation. After exceeding the previous maximum burial depth VR maturation continues. **Right:** Conceptual view of VR offset at erosional horizons. More burial and subsequent erosion leads to larger offsets in VR. This can be used to identify and calibrate major unconformities.

In absence of large VR data sets, Vitrinite Reflectance Equivalents (VRE) are derived from Jarvie et al. (2001)s empirical relation (equation (3.1)). This relation is based on type II marine kerogen measured in the Barnett Shales found in the USA. T_{max} corresponds to the temperature at which kerogen thermal breakdown peaks (Allen and Allen, 2013). The Jarvie et al. (2001) algorithm should only be used if the Barnett Shale can be used as an analogue, but in practice this relation is widely used for source rocks containing type II kerogen (Soua, 2014b; Wust et al., 2013).

$$VRE = 0.180 \times T_{max} - 7.16 \tag{3.1}$$

The Fegaguira Shales and its Hot Shale member contain type II kerogen deposited in marine environment, making the Barnett Shales an appropriate analogue (Soua, 2014b). VRE values computed with Jarvie et al. (2001)s empirical relation (equation (3.1)) show a good correlation with VR measurements from wells in the area of interest (figure 3.3). Especially in wells SB-1, SB-4 and SB-6 the VRE values fit well with measured VR (location in figure 3.5). This fortifies the confidence in the use of Jarvie et al. (2001)s empirical relation for calibration of the thermal and tectonic history in the area of interest.

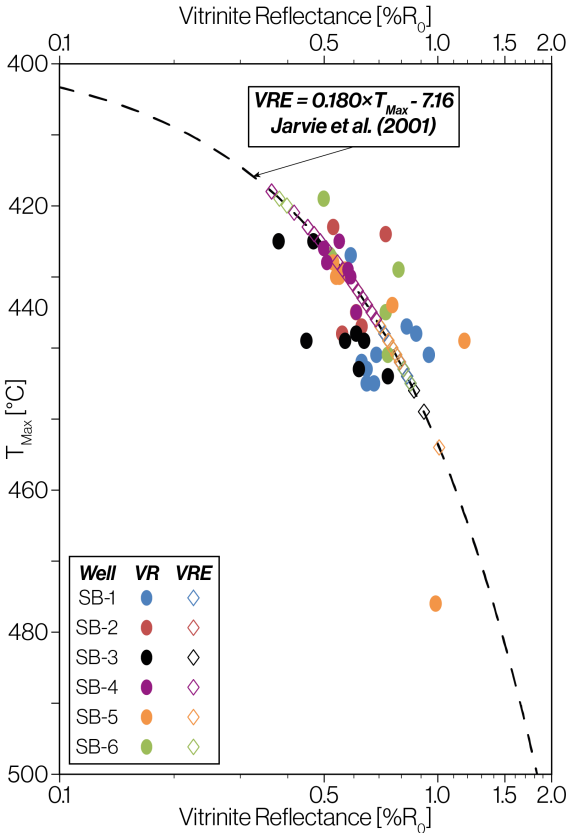

Figure 3.3: VRE and VR vs T_{max} per well in the area of interest. VRE values computed with Jarvie et al. (2001)s empirical VRE – T_{max} relation (equation (3.1)). The computed VRE values provide a reasonable fit with the VR measurements obtained from well data.

3.2 BURIAL HISTORY MODEL

As a sediment package is buried, subsequent deposition of basin-fill results in additional loading. This results in mechanical compaction of underlying formations, reducing their thickness (Lee et al., 2019). Tectonic phases such as shortening, tilting and basin inversion also affect the basin-fill and may result in exhumation and erosion. Therefore, the present-day stratigraphic column is not necessarily representative of formation paleo-thicknesses (Allen and Allen, 2013; Lee et al., 2019).

Unconformities in the present-day stratigraphy are associated with large uncertainties in terms of sediment erosion and can significantly impact timing of source rock maturation. Underdown et al. (2007) suggest that only the most significant unconformities in terms of exhumation have a major influence on source rock maturation and limited the burial histories to these unconformities.

Present-day stratigraphic columns (figure 3.4) provide information on formation age, thickness, and lithology and indicate time gaps. The burial history includes the major unconformities observed in seismics. Initial high and low case estimates of the amount

of eroded sediment associated with these unconformities are based on adjacent analogue basins, seismic lines and well data.

Each unit affected by the unconformity is assigned high and low case eroded sediment estimates, assuming equi-thickness deposition, to capture the uncertainties in low and high case 1D tectonic scenarios. The assigned amount of sediment is subsequently eroded during the exhumation phase associated with the unconformity. Decompaction, or *backstripping*, restores each formation to its paleo-thickness. This results in high and low case burial history scenarios which help constrain the impact of exhumation uncertainties on source rock maturation and hydrocarbon migration (Lee et al., 2019; Underdown et al., 2007). In addition to that, a "null" case with no erosion is decompacted to as a reference. Comparing the null case in the available wells in the area of interest helps investigating the subsidence behaviour throughout the area.

VR curves often have offsets at major erosional structures (figure 3.2), as uplifted formations experienced higher paleo-temperatures than the overlying formations (Hantschel and Kauerauf, 2009). If VR data sets capture such an offset it is possible to calibrate the burial history by means of a sensitivity analysis (Underdown et al., 2007). A range of erosion estimates associated with an unconformity is calibrated with VR and VRE data to further constrain the burial history scenarios and reduce uncertainties in subsequent maturation and migration studies.

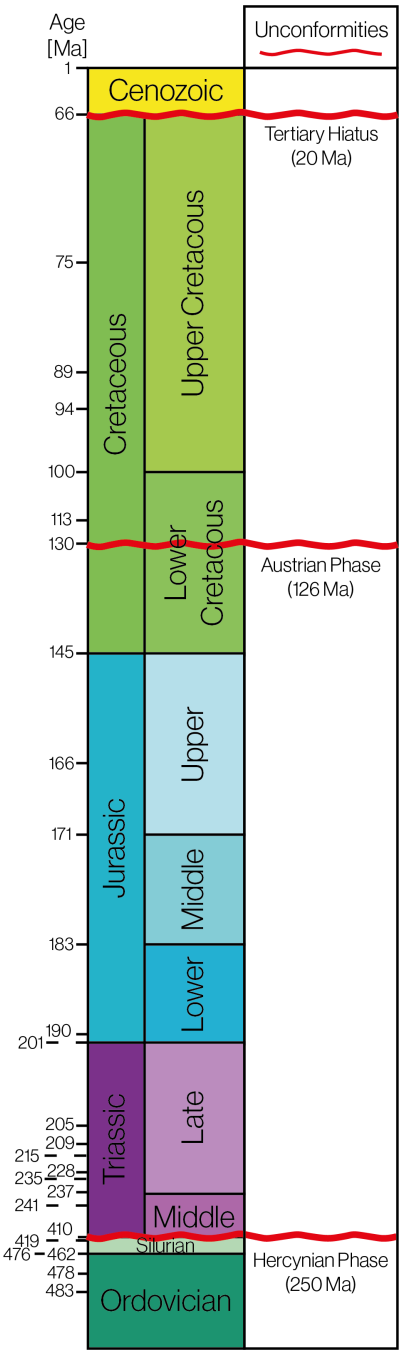

Figure 3.4: Synthetic present-day stratigraphic column based on well reports. Formation top age estimation is obtained from Bruna et al. (2019b) and Mejri et al. (2006)

3.3 BOUNDARY CONDITIONS

Model boundary conditions used for thermal modelling include paleo-Water Detph (PWD), Sediment-Water Interface Temperature (SWIT) and paleo heat flow (Bora and Dubey, 2015). Paleo-bathymetry data, i. e. paleo-water depth, is used for reconstruction of the basin subsidence (Underdown, 2006). The SWIT determines the paleo-surface temperature evolution through time (Wygrala, 1989). Both PWD and SWIT have minimal impact on modelling thermal maturation. Due to lack of paleo-bathymetry and paleo-surface temperature data in the Southern Chotts Basin, and their limited impact, PWD and SWIT input are neglected.

3.3.1 *Heat Flow Model*

Basin heat flow depends on a wide variety of parameters, e. g. stratigraphy thermal conductivity, lithosphere tectonics, surface temperature and heat generation from igneous bodies, and is challenging to define (Allen and Allen, 2013; Underdown, 2006). However, it considerably affects source rock maturation and hydrocarbon generation. Therefore a valid heat flow model is crucial in petroleum system modelling (Bora and Dubey, 2015).

Reconstruction of the thermal history in the basin requires definition of the present-day and paleo-heat flow (Yalçin et al., 1997). A range of present-day heat flows is calibrated with present-day subsurface temperatures, obtained with e. g. Horner correction of BHT measurements, which leaves one preferred present-day heat flow.

Studies of present-day and ancient geotherms suggest that thermal regime closely reflects tectonic history (Allen and Allen, 2013). Due to uncertain basin evolution during the Paleozoic, several paleo-heat flow models are synthesized, e. g. constant heat flow or tectonic based. Combined with the calibrated present-day heat flow, thermal maturation is modelled using Sweeney and Burnham (1990)s Easy%R_0 algorithm. The resulting maturation profiles are calibrated with VR and VRE data from the available wells in the area of interest. Thereafter one preferred heat flow model is selected for further source rock maturation modelling.

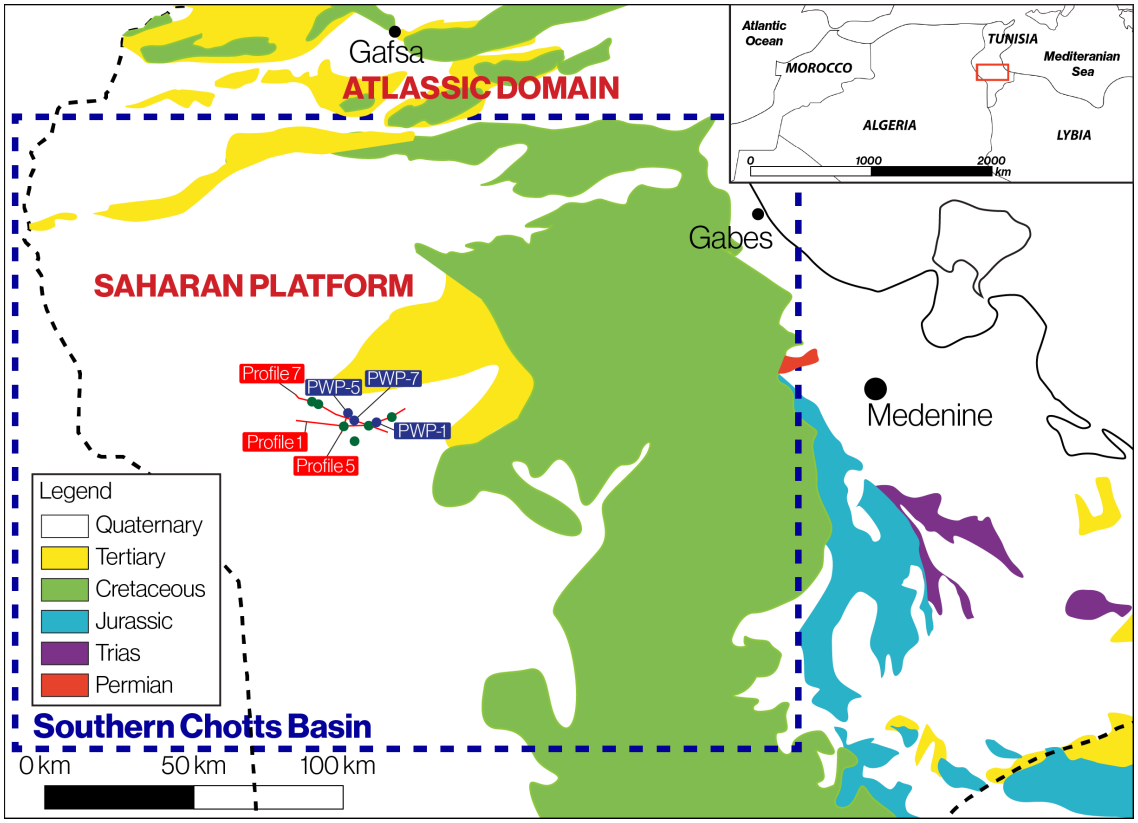

Figure 3.5: Location of pseudo wells (blue label) used to model source rock maturity in the structural lows in the area. The pseudo wells are placed along selected seismic profiles used for migration studies. Exploration and production wells used for calibration process are labeled in green. Amended from Bruna et al. (2019b).

3.4 SOURCE ROCK MATURATION & MIGRATION STUDIES

Exploration and production wells used for calibration of the migration model target trapped oil accumulations, generally located in structural highs. Structural lows have experienced deeper burial and are therefore more likely to host matured packages of source rock and function as the petroleum system *kitchen*. In absence of wells penetrating the potential kitchen area, several structural lows will be targeted with pseudo-wells (location in figure 3.5). Seismic data and interpretation allows construction of synthetic stratigraphic columns and burial histories. These pseudo-wells give insight in the source rock maturation history of the potential kitchen area and how expelled hydrocarbons in this region migrated towards present-day accumulations.

Previously calibrated thermal and synthetic burial histories are used to model VR and Transformation Ratio (TR) over time in the pseudo wells as part of a 1D source rock maturation study. TR indicates the portion of kerogen that is thermally decomposed and generated hydrocarbons. Its evolution over time indicates the timing and amount of hydrocarbon generation. However, high TR does not necessarily indicate that hydrocarbons have been preserved. Exhumation following deep burial may bring hydrocarbon bearing formations to the surface, causing them to leak (Magoon and Dow, 1994).

To investigate the effects of such periods of exhumation and see where generated hydrocarbons migrated to, we perform several migration studies along 2D seismic transects (figure 3.5). These transects cross the pseudo-wells and are oriented to capture the potential kitchen area and 3D architecture. The seismic transects used in the migration study have previously been depth converted in a study conducted by Bruna et al. (2019a). The important petroleum system elements, i. e. potential reservoir, source and seal rocks are interpreted from these 2D transects and form the sediment packages in the migration model. In absence of detailed reservoir rock lithofacies distribution, appropriate default lithofacies characteristics are assigned to these sediment packages. Source rock parameters are assigned based on geochemical data from wells in the area of interest (location in figure 3.5). The influence of the depositional environment of important reservoir rocks is evaluated during interpretation of potential sweet spots.

The depth converted sections are restored through time by means of backstripping according to the calibrated burial histories to investigate the migration pathways at important times in the petroleum system evolution (e. g. pre- and post-exhumation, after deposition of the cap rock). Comparing the simulated present-day accumulations with hydrocarbon discoveries in wells helps selecting an overall preferred model. This preferred model offers insight in e. g. hydrocarbon spills, carrier beds, unexpected migration pathways, source location, and potential sweet spots.

4 EXHUMATION INVESTIGATION

Seismic data in the area of interest shows seismic reflectors dipping NE in the Ordovician – Early Devonian sequence are truncated by SW dipping reflectors in the Triassic TAGI Formation (figure 4.1). This indicates that the Ordovician – Early Devonian sequence is unconformably overlain by the Triassic package, and the Early Devonian – Permian sequence is missing throughout the area of interest. This corresponds to a time gap in the depositional sequence of at least 160 Ma.

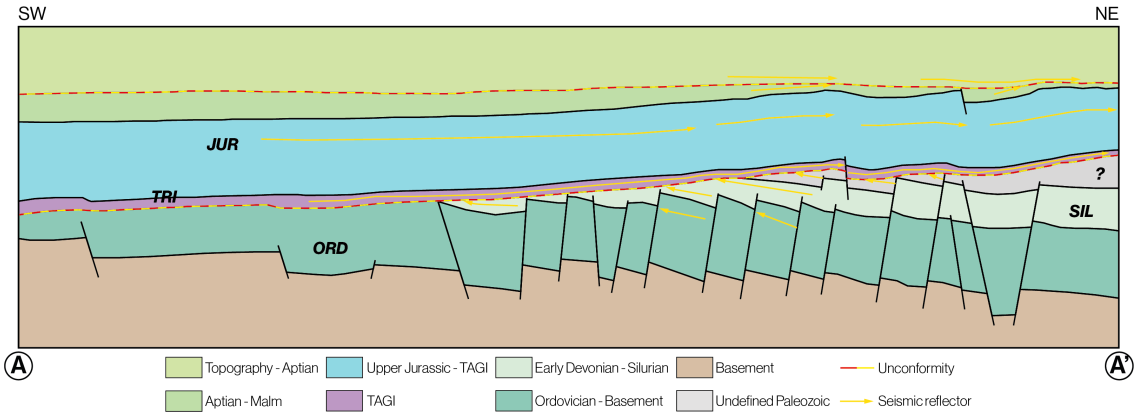

Figure 4.1: NE–SW seismic line capturing the present-day structure of the Southern Chotts basin (location in figure 2.1). Seismic reflectors in Paleozoic package are truncated by the Triassic TAGI. Absence of the Devonian – Permian sequence in the seismic data prohibits thickness estimation of these packages.

Well SB-1 shows an offset in vitrinite reflectance at the unconformable contact between the Silurian – Early Devonian and Triassic deposits (figure 4.2). The Paleozoic units experienced higher temperatures and maturation than the unconformably overlying Mesozoic units. This indicates that the area of interest experienced further burial after deposition of the Early Devonian – Silurian package, increasing the maturation of this unit. Subsequent removal of the deposited overlying sediments prior to deposition of the Triassic package results in this VR offset. This eliminates the possibility of non-deposition during the Early Devonian – Permian period. Therefore, the area of interest experienced deposition of (part of) the Early Devonian – Permian sequence, prior to uplift and erosion of the deposited sediments. Frizon de Lamotte et al. (2013) and Galeazzi et al. (2010) argued that the Telemzane Arch influ-

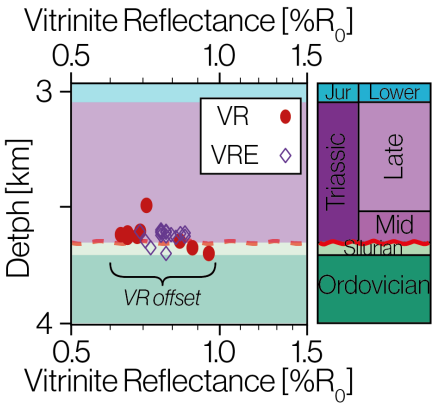

Figure 4.2: Offset in vitrinite reflectance data at the Hercynian unconformity in well SB-1 in the area of interest. This indicates that the Paleozoic units experienced further burial and subsequent uplift prior to deposition of the Mesozoic units.

enced sediment deposition in the adjacent basins during this period. Galeazzi et al. (2010) also argued that Late Paleozoic erosion and deformation led to the removal of large intervals of Paleozoic deposits in the vicinity of the Telemzane Arch. Investigating the depositional environment in these adjacent basins helps estimate the amount of sediment deposited during the Early Devonian – Permian that has subsequently eroded. Galeazzi et al. (2010) presented a pre-Mesozoic subcrop map of the Hercynian unconformity, indicating the distribution of Paleozoic deposits with respect to the Telemzane Arch and suggesting where to investigate the missing deposits (figure 4.3).

4.1 ESTIMATION OF INITIAL DEPOSITION

Silurian & Ordovician

The Silurian – Early Devonian deposits are present throughout the area of interest, but seismic data shows that these units have experienced partial erosion in the area of interest (figures 4.1 & 4.4). The internal reflectors of the Silurian – Early Devonian and underlying Ordovician packages indicate that their thickness is relatively constant if not truncated by the Hercynian unconformity. These seismic transects, oriented in N – S direction (figure 2.1), show truncation of the Ordovician and Silurian – Early Devonian packages occurs towards Telemzane Arch. Frizon de Lamotte et al. (2013) argue that the Telemzane Arch was not a significant regional high until the Late Devonian. Therefore, it is a reasonable assumption that these packages were deposited at constant thickness prior to exhumation. This allows the projection of a constant initial thickness throughout the area of interest.

The Ordovician package seems to have experienced only minimal erosion throughout the area of interest and is generally overlain by the Early Devonian – Silurian package (figure 4.1 & 4.4). The maximum thickness of the Silurian – Early Devonian package encountered throughout the area of interest is ca. 430 m in well SB-3, bounded above by Triassic deposits. The minimum thickness, if not completely eroded, is ca. 50 m in well SB-1. Therefore the estimated minimum and maximum initial thicknesses are 100 and 400 m respectively.

Devonian & Carboniferous

Frizon de Lamotte et al. (2013) showed that in the Hassi R'Mel area and Jeffara basin the Devonian and Carboniferous likely deposited in an extensional regime north and south of the Telemzane Arch. However, the Devonian is removed north of the arch during a Late Devonian exhumation phase (Frizon de Lamotte et al., 2013). The Southern Chotts basin is located on a similar location with respect to the Telemzane Arch, in between the Hassi R'Mel area and Jeffara basin (figure 4.3). Therefore we argue the area experienced similar deposition and removal of the Devonian sequence followed by deposition of the Carboniferous related to post rift sag (Frizon de Lamotte et al., 2013).

Carboniferous thicknesses found north of the Telemzane Arch serves as adequate initial estimates for the deposited package in the Southern Chotts basin. In the Jeffara basin, wells KR-1 and LG-1 report ca. 550 m op the complete Carboniferous sequence in close proximity to the Telemzane Arch, while further away from the arch well MA-1 reports 900 m of Carboniferous (figure 4.3) (Mejri et al., 2006). Considering the similar distance to

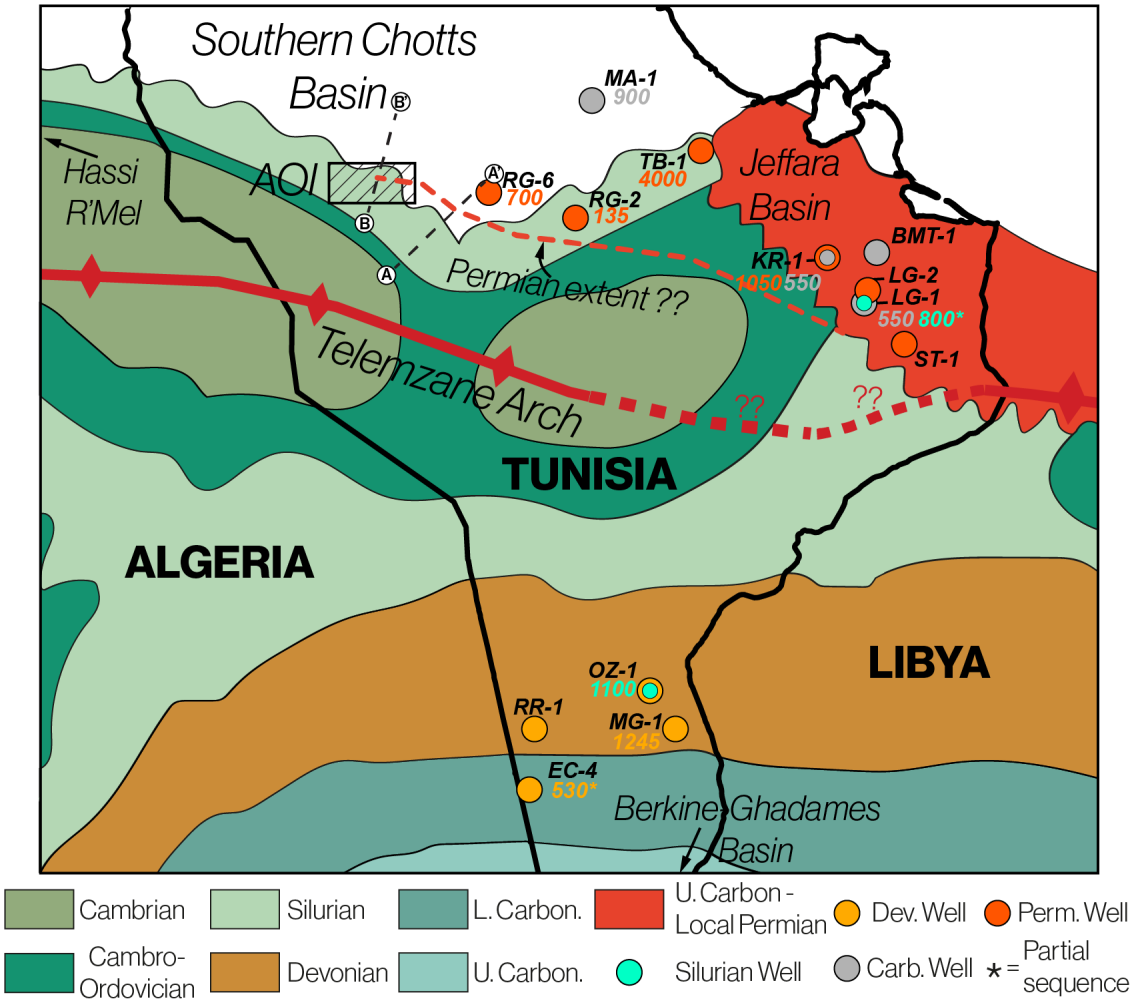

Figure 4.3: Pre-Mesozoic subcrop map of the Hercynian unconformity in the basins adjacent to the Telemzane Arch, ammended from Galeazzi et al. (2010). Thicknesses of Silurian, Devonian, Carboniferous and Permian well discoveries documented by Mejri et al. (2006) are shown on the map. The extent of the undefined Paleozoic package interpreted from seismics (figures 4.1 & 4.4) marks the possible extent of the Permian terrestrial deposits.

the Telemzane Arch as wells KR-1 and LG-1, the estimated thickness of the Carboniferous deposits in the Southern Chotts basin is ca. 400 – 700 m (Bruna et al., 2019a).

Due to absence of Devonian sediments north of the arch, we resort to Devonian thicknesses reported south of the Telemzane Arch for initial estimation of the amount of deposited Devonian in the Southern Chotts basin. In the Berkine – Ghadames basin, well MG-1 penetrates the complete Devonian series and shows a maximum Devonian thickness of ca. 1250 m. The Upper Devonian makes up ca. 530 m of this sequence, as shown in well EC-4 (figure 4.3) (Mejri et al., 2006). Considering the Late Devonian – Early Carboniferous exhumation north of the Telemzane Arch (Frizon de Lamotte et al., 2013), Late Devonian deposition in the Southern Chotts basin is uncertain. Therefore, we consider an initial estimated Devonian thickness is 500 – 1200 m.

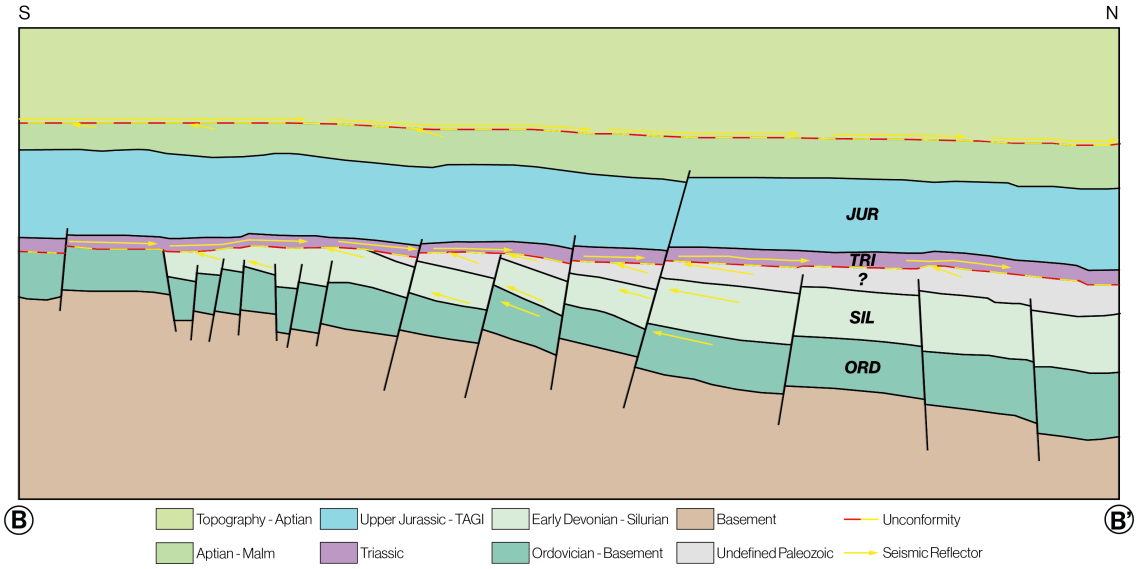

Figure 4.4: N-S seismic line roughly perpendicular to the Telemzane Arch passing through the area of interest (location in figure 2.1. Seismic reflectors Ordovician and Early Devonian – Silurian package show these packages are relatively constant in thickness if not truncated by the Hercynian unconformity.

Permian

Zaafouri et al. (2017) interpreted the preserved Permian sequence in the Jeffara basin to be deposited in a roughly WNW – ESE trending carbonate shelf system prograding northwards. The deposits of this sequence change laterally from deep marine shales (TB-1) to reef carbonates, shallow marine carbonates, and clastics towards the landward located Telemzane Arch (Frizon de Lamotte et al., 2013; Zaafouri et al., 2017).

Seismic lines in the vicinity of the area of interest (figures 4.1 & 4.4) show a package of undefined Paleozoic deposits truncated by the Hercynian unconformity extending WNW – ESE (figure 4.3). Well RG-2 and RG-6 record Permian sand deposits, suggesting Permian deposits extend in the northern part of the area of interest, just outside the 3D seismic block. This argues deposition of a clastic Permian sequence in the area of interest, in contrast to the marine deposits in the Jeffara basin. This landward position makes the area of interest more prone to erosion during a Late Permian exhumation phase and could explain why the Permian is generally absent in the Southern Chotts basin but is well preserved in the Jeffara Basin.

Well RG-6 reports 700 m of Permian deposits and indicates that significant amounts of Permian deposits were initially deposited in the area of interest. The lack of well control on the undefined Paleozoic package identified in the seismic lines (figure 4.1 & 4.4) makes estimation of Permian thickness using seismics uncertain. Therefore, initial estimates are adapted from Mejri et al. (2006), who estimate the Permian thicknesses ranges between 400 – 1000 m, and will be calibrated with VR data.

4.2 IMPLEMENTATION IN TECTONIC HISTORY

Despite our efforts to estimate amount of initially deposited Paleozoic sediment, the absence of the Devonian – Permian units results in considerable timing and erosion uncertainties in the tectonic history. To resolve this problem, we resort to calibrating the amount of eroded Paleozoic sediment with the offset in VR and VRE data (figure 4.2) (Underdown et al., 2007). In combination with the present-day thickness of the eroded units this indicates the minimum and maximum amount of sediment deposited during the Paleozoic. This serves as input for a calibrated high and low case burial history that allows to investigate whether the source rock matures significantly prior to Hercynian exhumation in the subsequent maturation study. **Note** that there is an emphasis on Hercynian exhumation as it presents the largest unconformity in the area. The amount of eroded material associated with this phase may result in premature generation and significant hydrocarbon leaking.

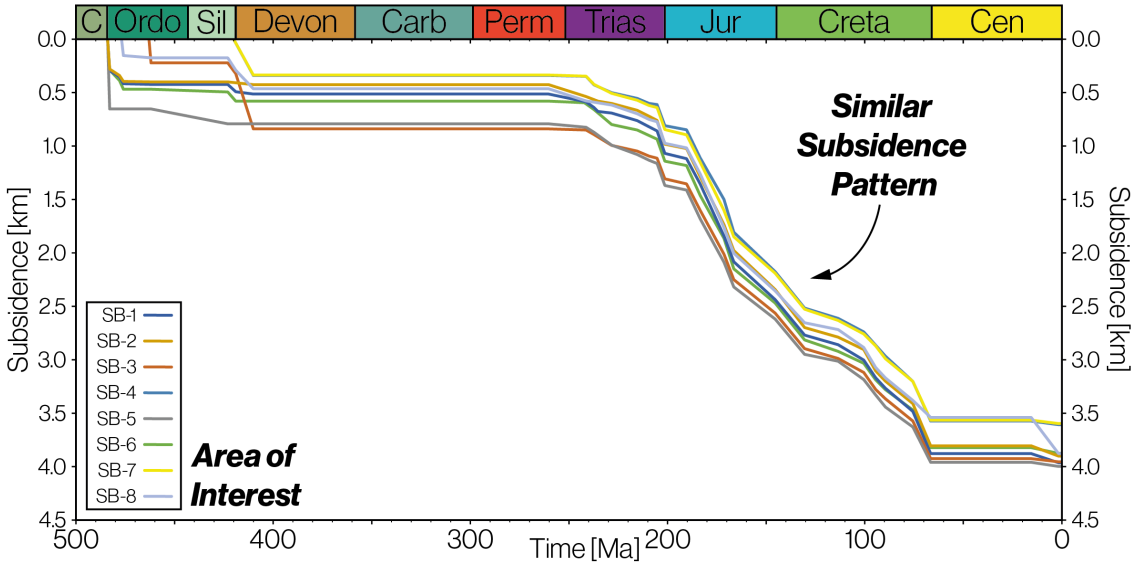

Figure 4.5: Subsidence analysis of the wells in the area of interest by means of subsequent decompaction of the stratigraphic column. The subsidence pattern is similar throughout the area of interest since the Mesozoic, i. e. ca. 250 Ma. This implies the area of interest experienced relatively constant sediment deposition.

Since the Early Devonian – Permian sequence is absent in wells in the area of interests, no direct indications on subsidence in this period can be obtained from decompaction and subsidence analysis. However, the subsidence patterns since the Mesozoic, i. e. for ca. 250 Ma, are very similar (figure 4.5). This suggests that the subsidence and depositional behaviour are relatively constant throughout the area of interest over the past 250 Ma. In absence of data on Paleozoic subsidence behaviour in the study area, we argue that the amount of sediment deposited throughout the area of interest is also relatively constant during the Early Devonian – Permian. The thicknesses of the Ordovician and Early Devonian – Silurian packages observed in seismic data supports this argument (figures 4.1 & 4.4). Therefore, the VR calibrated amount of eroded Paleozoic sediment, and the associated amount of Paleozoic deposition, is projected at constant thickness throughout the area of interest.

It is important to note some misleading features in this subsidence analysis. The thickness of the lowermost unit is not the true thickness, since the bottom of the unit is not encountered. Similarly, e. g. well SB-7 seems to experience ”less subsidence”, while in reality the well simply does not penetrate the Ordovician package. In addition to this, the start of deposition is taken to be the top age of the lowermost unit, such that depositional rate is not wrongly implied. This is visible in the near vertical portions of the subsidence curves in the Ordovician – Silurian, since most wells terminate in these units.

5 RESULTS

5.1 SOURCE ROCK GEOCHEMISTRY

Bora and Dubey (2015) suggest that the Central Arabian Silurian Qusaiba hot shales, containing type II kerogen, serve as an appropriate analogue for Silurian hot shales in Tunisia. Abu-Ali et al. (1999) conducted kerogen compositional thermal degradation experiments on samples from the Qusaiba hot shale to simulate the maturation process. The experimental results were combined with regional source rock depth maps to model generation and expulsion. This indicated that timing of kerogen transformation and hydrocarbon expulsion differ. Abu-Ali et al. (1999) captured this in a publicly available custom kinetic model for the Qusaiba hot shales. In absence of kerogen kinetic data for the Fegaguira and Hot Shales, the Quasaiba hot shales will serve as an analogue.

5.2 BURIAL HISTORY MODEL

Upon investigating seismics data (figures 4.1 & 4.4) and the stratigraphic column (figure 3.4) in the area of interest, 3 time gaps are identified in the area of interest and its surroundings:

1. Hiatus between Pliocene – Quaternary and Upper Cretaceous ("Tertiary hiatus")
2. Aptian deposits overlying the Upper Jurassic ("Austrian unconformity")
3. Triassic unconformably overlying Ordovician – Early Devonian deposits ("Hercynian unconformity")

Seismic data in the area of interest (figure 4.4) does not show a distinctive unconformable contact between the Aptian and Upper Jurassic. However, east of the area of interest (figure 4.1) the Aptian is found unconformably overlaying the Upper Jurassic. The close proximity to the area of interest indicates an exhumation as late as the start of the Aptian should be considered.

Investigation of seismic data and adjacent analogue basins resulted in initial estimates for the amount of sediment deposited during the Silurian – Permian (chapter 4). A low and high case burial history scenario is proposed to capture the erosion uncertainties with the following assumptions:

- During to the Austrian and Hercynian phase the area of interest experienced erosion of previously continuous deposited sediment
- The amount of eroded sediment is based on high and low case estimates proposed in chapter 4
- Amount of Paleozoic sediment deposition is calibrated with VR and VRE data

- Early Devonian – Permian sediments eroded during a single phase of Hercynian exhumation in the Late Permian – Early Triassic (ca. 260 – 250 Ma)
- Lower Cretaceous sediments deposited prior to Aptian eroded during a single phase of Austrian exhumation prior to the Aptian (ca. 130 – 126 Ma)
- No sediment deposition occured during the Tertiary hiatus (ca. 66 – 20 Ma)
- Units are assigned default formation lithology based on the present-day stratigraphic column
- The sediment units are compacted by subsequent loading, which is accounted for with backstripping
- Additional Null Case scenario without erosion for comparison

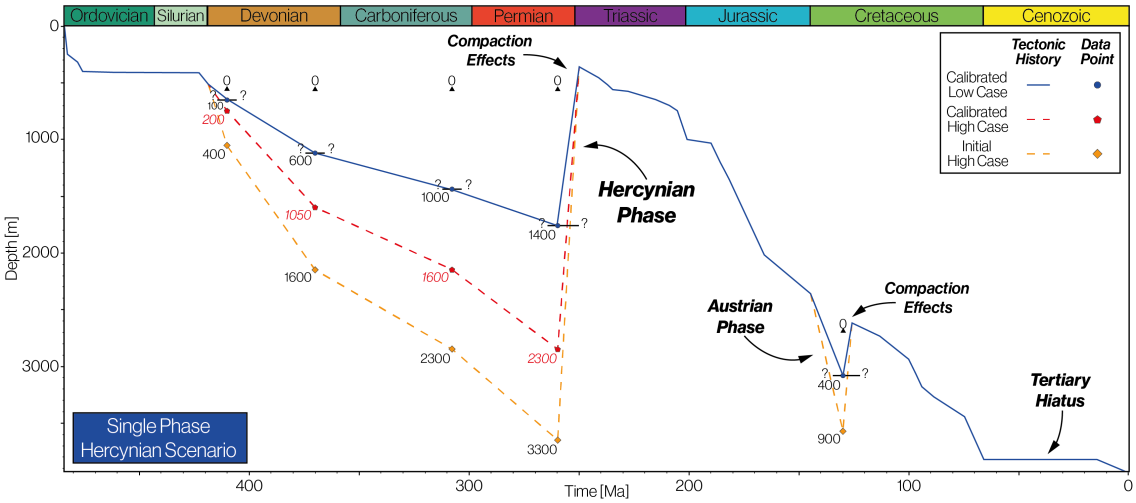

Figure 5.1: Burial history scenarios regarding a single Hercynian exhumation phase at the Late Permian – Early Triassic. Eroded sediments are initially deposited with homogeneous thickness in the area of interest. Null case assumes no erosion and therefore experienced less compaction. Burial history is calibrated with VR and VRE data using a sensitivity analysis (figure 5.2).

The proposed burial history scenarios depict the range of vertical movements throughout the area of interest (figure 5.1). Slight confusion may be caused by differences in burial depth following an exhumation phase, e. g. at ca. 250 Ma, for the different scenarios. More sediment deposition prior to exhumation leads to more heavily compacted units, and therefore shallower burial depth once exhumation concludes. This difference is especially noticeable in comparison with the null case, which experienced no additional compaction prior to exhumation (figure 5.1). This does not affect the present-day stratigraphic column.

Sensitivity analysis on the maximum Hercynian burial depth and calibration with VR and VRE data from the area of interest minimizes the exhumation uncertainties. Well SB-1 contains the most distinct offset in VR measurements between the Paleozoic and Mesozoic sediment package (figure 5.6), serving as the primary data source for maximum burial depth calibration. Accurate calibration between modelled VR and experimental VR data is achieved for an additional Paleozoic sediment thickness between 0 – 2300 m, indicating that the area of interest experienced a maximum of 2300 m of Hercynian erosion (figure 5.2). Consequently, we propose a new "calibrated high case" burial history scenario, including this maximum Paleozoic burial, for further modelling (figure 5.1).

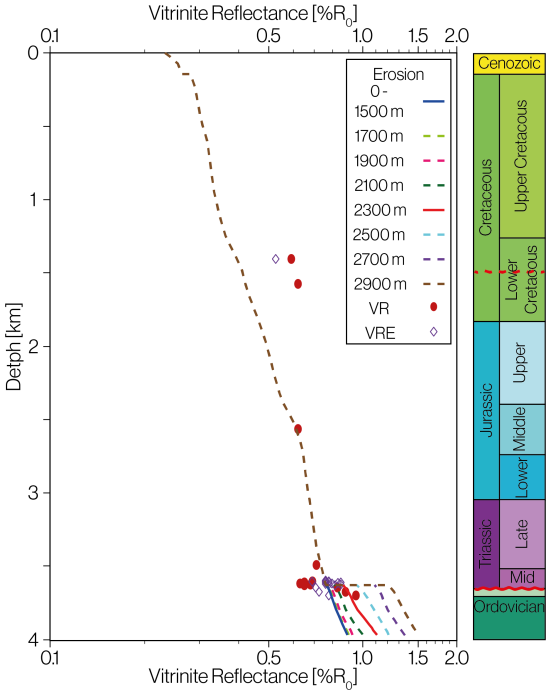

Figure 5.2: Calibration of maximum Hercynian burial depth with VR and VRE measurements, by means of sensitivity analysis over a range of 0 – 2900 m. Accurate calibration is achieved using Hercynian maximum burial depths up to 2300 m.

Subsidence analysis emphasized that all wells in the area of interest show similar subsidence patterns during the Mesozoic (figure 4.5). Therefore, it is reasonable to assume that similar amounts of Silurian – Permian sediment deposited throughout the area of interest and has subsequently eroded. This implies that the calibrated amount of sediment eroded during the Hercynian phase (figure 5.2) is valid throughout the area of interest. Applying the calibrated tectonic scenarios in the remainder of the wells in the area of interest also gives a reasonable fit with VR and VRE measurements (figures 5.5 & 5.6).

5.3 HEAT FLOW MODEL

Available corrected BHT and corresponding TSLC measurements allowed calibration of simulated present-day temperature profiles by means of sensitivity analysis (figure 5.3). From a range of present-day constant heat flows, the simulated subsurface temperature profile corresponding to a heat flow of 60 mW m^{-2} fits best with BHT data. Therefore, 60 mW m^{-2} is used as the preferred present-day heat flow in the remainder of the thermal history models.

A total of 6 paleo heat flow models are proposed based on constant heat flow (scenario 1), the tectonic history of the Southern Chotts Basin (scenarios 3 – 5), and previous studies (scenario 2 & 6) by Derguini et al. (2005) (figure 5.4). Input for the tectonic history scenarios is based on typical heat flow ranges for sedimentary basins from Allen and Allen (2013). The key input for the tectonic scenarios are: 1) moderate heat flows during Cambro – Ordovician times (Derguini et al., 2005), 2) compression during the Hercynian phase, 3) volcanic activity indicated by deposition of igneous rocks during the Triassic,

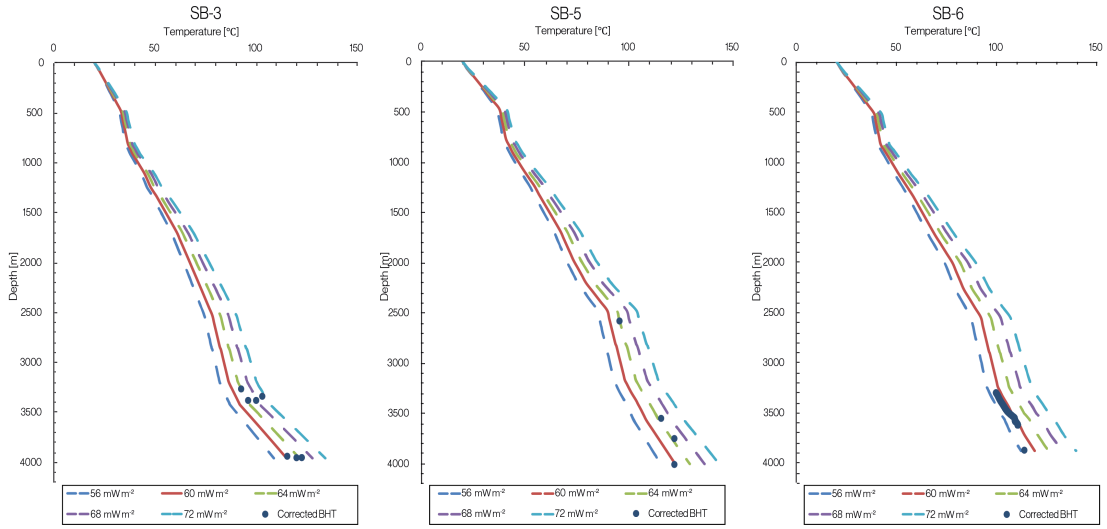

Figure 5.3: Calibration of present-day temperature profiles with available corrected BHT data from the area of interest. The preferred present-day heat flow is 60 mW m^{-2}.

4) continued Mesozoic extension interrupted by Austrian Phase, and 5) the calibrated present-day heat flow.

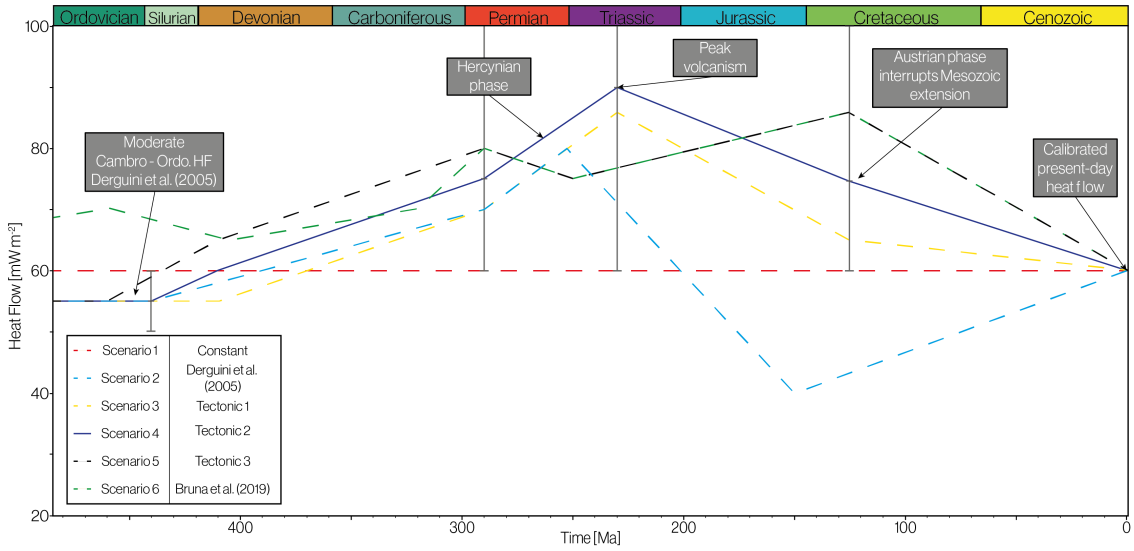

Figure 5.4: Proposed heat flow scenarios to be calibrated with vitrinite reflectance data from the selected wells. Scenarios are based on constant heat flow, tectonic history and Derguini et al. (2005). Tectonic scenarios based on heat flow estimates amended from Allen and Allen (2013) and Derguini et al. (2005).

Modelled Easy%R_o curves corresponding with the heat flow scenarios are calibrated with VR and VRE measurements for the calibrated low and high case tectonic histories (figures 5.5 & 5.6). Generally, in the tectonic low case scenarios 1 and 2 underestimate VR measurements, scenarios 3 and 4 align with the data, and scenarios 5 and 6 overestimate VR. Calibration of the heat flow scenarios in the tectonic high case show similar results, where heat flow scenarios 3 and 4 align the best with the data throughout the whole area of interest. Overall, heat flow scenario 4 provides the best fit throughout the whole strati-

graphic column when considering both the calibrated low an high case tectonic history. Therefore, heat flow scenario 4 offers an accurate representation of the thermal history in the pseudo wells used in subsequent thermal maturation and migration studies.

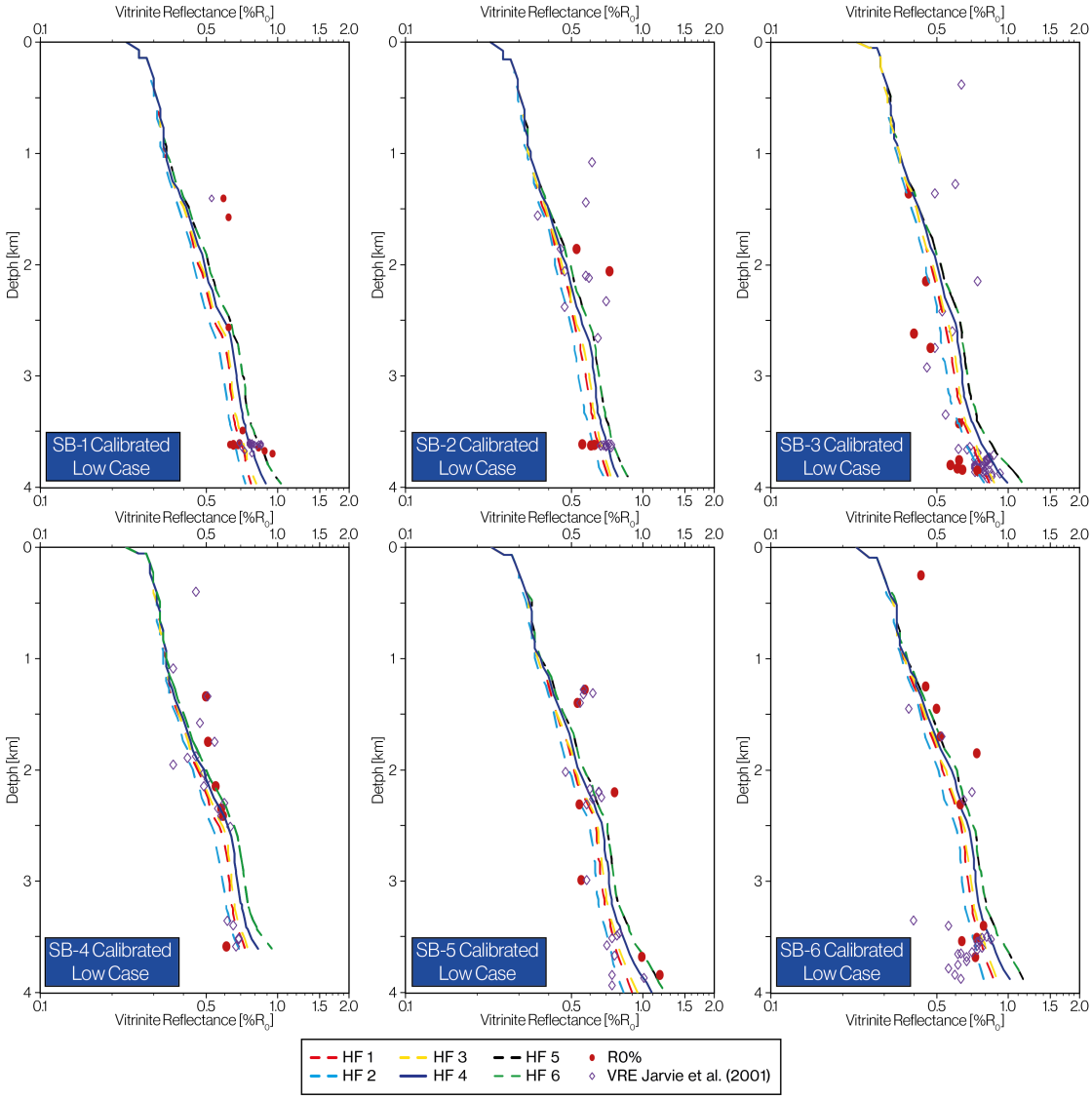

Figure 5.5: Calibration of Easy%R_o curves, corresponding to proposed paleo-heat flow models (figure 5.4), with VR and VRE in the available wells in the area of interest for the calibrated low case tectonic history. VRE is computed with the VRE – T_{max} relation by Jarvie et al. (2001) (equation (3.1)). Well locations in figure 3.5.

5.4 SOURCE ROCK MATURATION STUDY

Vitrinite reflectance and transformation ratio modelled for the calibrated burial histories in the available wells indicate that source rock maturation history varies significantly with burial history scenario, influencing both timing and level of maturation (figure 5.7). Maturation in the area of interest occured in 3 main stages; i. e. (1) progressively increasing

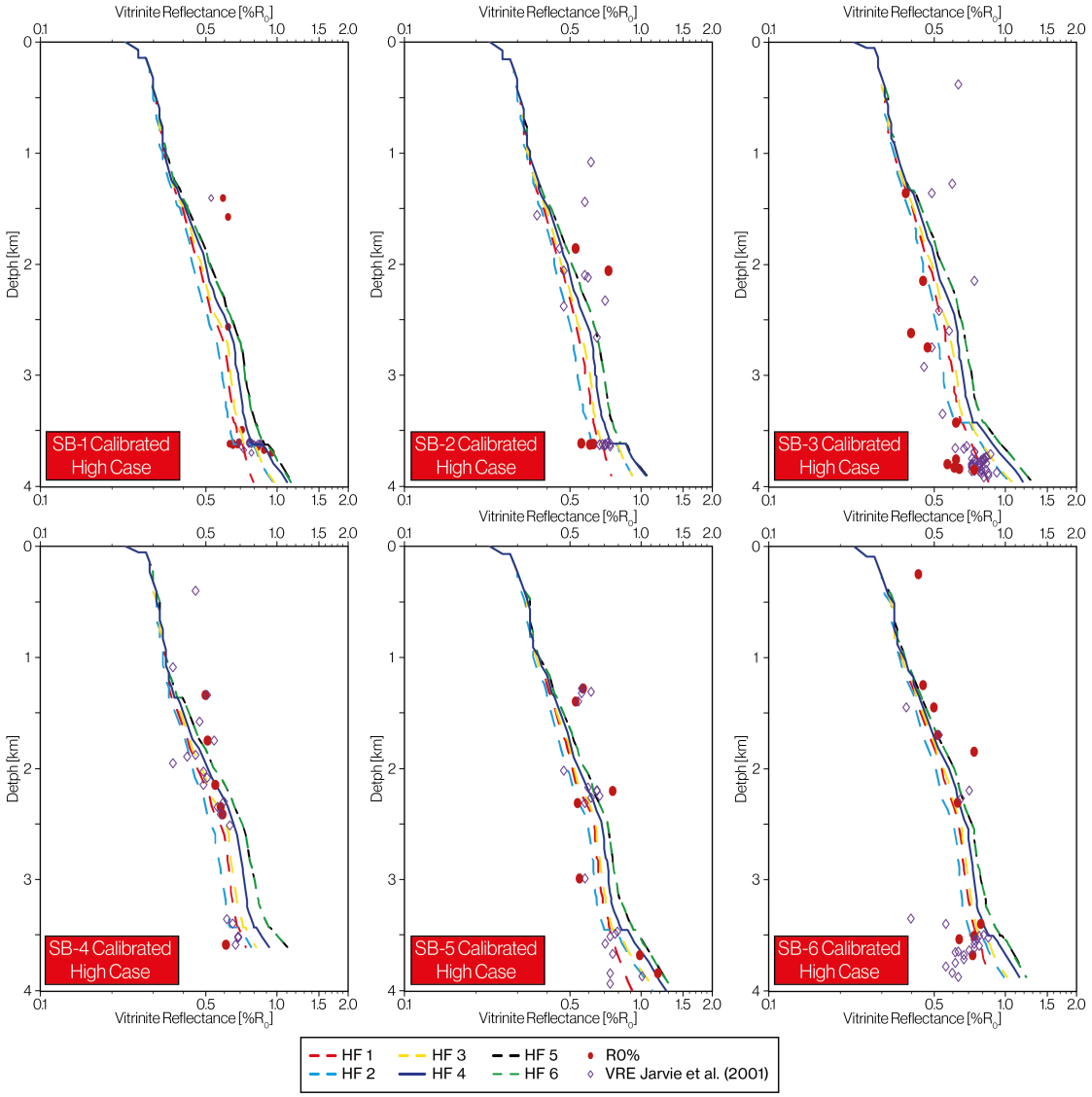

Figure 5.6: Calibration of Easy%R_o curves, corresponding to proposed paleo-heat flow models (figure 5.4), with VR and VRE in the available wells in the area of interest for the calibrated high case tectonic history. VRE is computed with the VRE – T_{max} relation by Jarvie et al. (2001) (equation (3.1)). Well locations in figure 3.5.

maturation rates in the Paleozoic, (2) stable maturity after Hercynian exhumation, and (3) renewed maturation after pre-Hercynian burial depth is exceeded in the Mesozoic.

The timing of stage (2) and (3) directly relates to the amount of Hercynian burial in the area of interest. Maturation is an irreversible process and only proceeds once previous experienced temperatures are exceeded, and therefore depends on the thermal and burial history. Assuming larger pre-Hercynian burial depths increases modelled maturation prior to exhumation and therefore the time it takes for Mesozoic burial to exceed previous maturation levels. This extends stage 2 and postpones stage 3. This directly reflects in the kerogen transformation and therefore hydrocarbon generation.

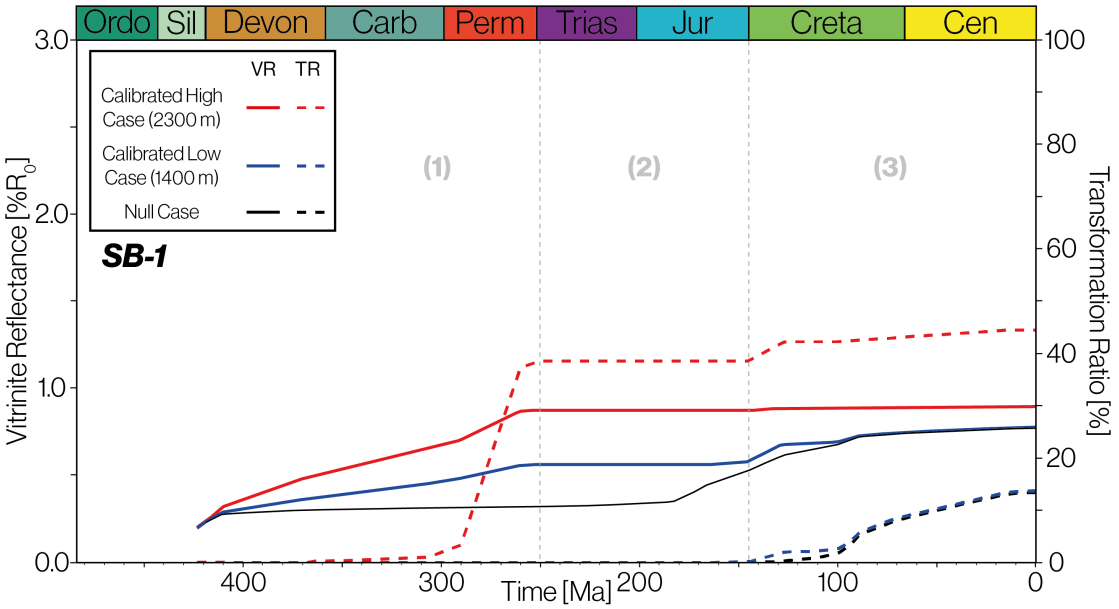

Figure 5.7: Modelled Hot Shales Vitrinite reflectance and transformation ratio in well SB-1 for the calibrated burial history scenarios. Maturation occurs in 3 stages, whose timing relate to pre-Hercynian maximum burial depth.

This trend is not visible in the pseudo wells, where renewed maturation starts simultaneously in all scenarios (figure 5.8). The stratigraphic column in the pseudo wells is interpreted from seismics rather than from well logs. As a consequence, the synthetic stratigraphic column contains has a low temporal resolution and fails to capture the same deposition history as the well logs. However, this does not influence the level of maturation and transformation modelled in the pseudo wells.

The potential kitchen area (well PWP-5, figure 5.8) shows similar stages of source rock maturation as well SB-1 (figure 5.7) for the calibrated burial histories. However, the source rock in well PWP-5 experiences increased maturation due to deeper burial (figure 5.8). This also reflects in the kerogen transformation, indicating the structural lows generated more hydrocarbons. The end of the Cretaceous marks decreased maturation, corresponding to the Tertiary Hiatus in the burial history.

The Silurian – Early Devonian source rocks entered the condensate and wet-gas zone (ca. 1.2 $\%R_o$) prior to Hercynian exhumation for the calibrated high case. A strong increase in maturation rate can be observed in during the Permian and results from increased burial rate and heat flow during this time. Mesozoic reburial further matures the source rock but remains in the condensate and wet-gas zone (ca. 1.45 $\%R_o$).

In the calibrated low case the Silurian – Early Devonian source rocks just reaches the oil window as generation starts in the Permian (ca. 0.8 $\%R_o$). An increase in maturation rate is observed during the Permian, although less drastic than in the high case due to a lower burial rate. Renewed maturation during the Mesozoic further matures the source rock, reaching the condensate and wet-gas zone (ca. 1.4 $\%R_o$).

To stress the importance of calibrating the amount of eroded material associated with major unconformities, we modelled maturation for the initial high case burial history. Besides not corresponding with VR and VRE data, overestimated amounts of erosion also have large implications for the maturation and generation history. The source rock

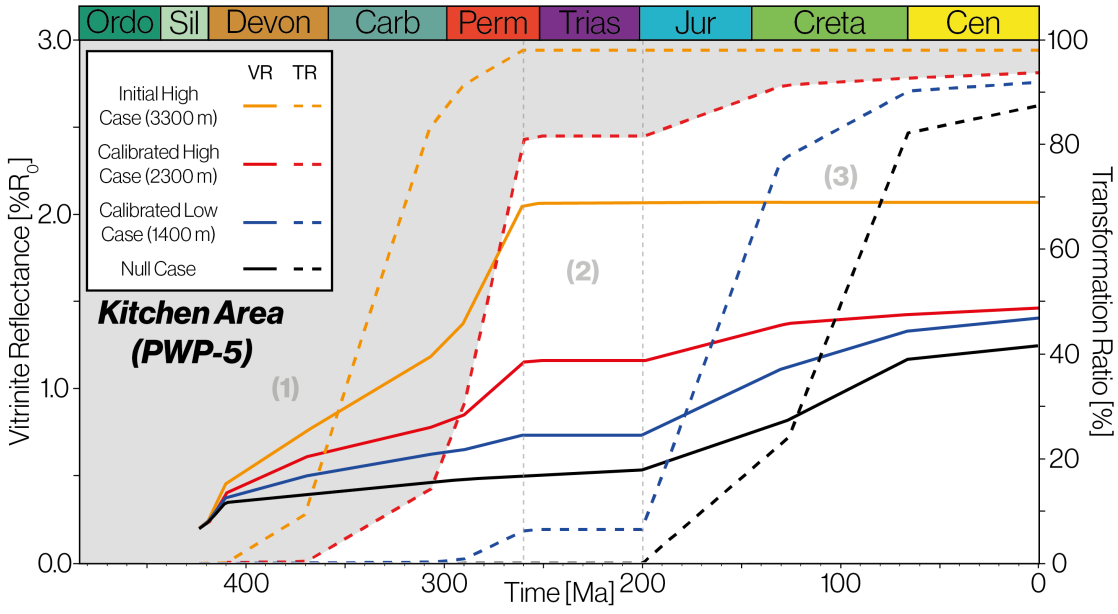

Figure 5.8: Modelled Hot Shales vitrinite reflectance and transformation ratio in the potential kitchen area (PWP-5) for the calibrated and initial burial history scenarios. Amount of erosion associated with Hercynian exhumation is noted for each case. The calibrated burial histories show 4 stages of maturation. Initial hydrocarbon generation occurs as early as the Paleozoic, leaving generation potential for renewed generation in the Mesozoic.

fully matures prior to Hercynian exhumation, therefore reaching its generation potential prior to deposition of an important cap rock, e. g. Triassic salt. This significantly increases the probability of trap breaches and hydrocarbon leaking. Hydrocarbons therefore are less likely to have preserved, which does not fit with present-day petroleum discoveries.

Hydrocarbon generation in the potential kitchen area (PWP-5) starts prior to the Hercynian exhumation (figure 5.8). The calibrated high case reaches a TR of ca. 80% prior to Hercynian exhumation, while the low case reaches ca. 10% leaving significant generation potential for the Mesozoic. This indicates the high case is dependent on Paleozoic generation, while the low case depends more on Mesozoic generation. Therefore the implications of Hercynian exhumation are larger for the high case, as more hydrocarbons may leak when charged formations come to the surface. It also implies that the high and low case burial histories experienced a different charging history, potentially migrating to different hydrocarbon accumulations.

5.5 MIGRATION STUDY

Migration from the potential kitchen area to potential reservoirs is simulated for the burial scenarios along NNE – SSW oriented profile 5 (figure 5.9). The important petroleum system elements are interpreted on this previously depth converted seismic transect by Bruna et al. (2019a). These sediment packages are assigned lithology characteristics and are decompacted through time according to the calibrated burial histories to give insight in the migration history. Due to seismic resolution the Ordovician Jeffara and Hamra units are merged into the "Ordovician units".

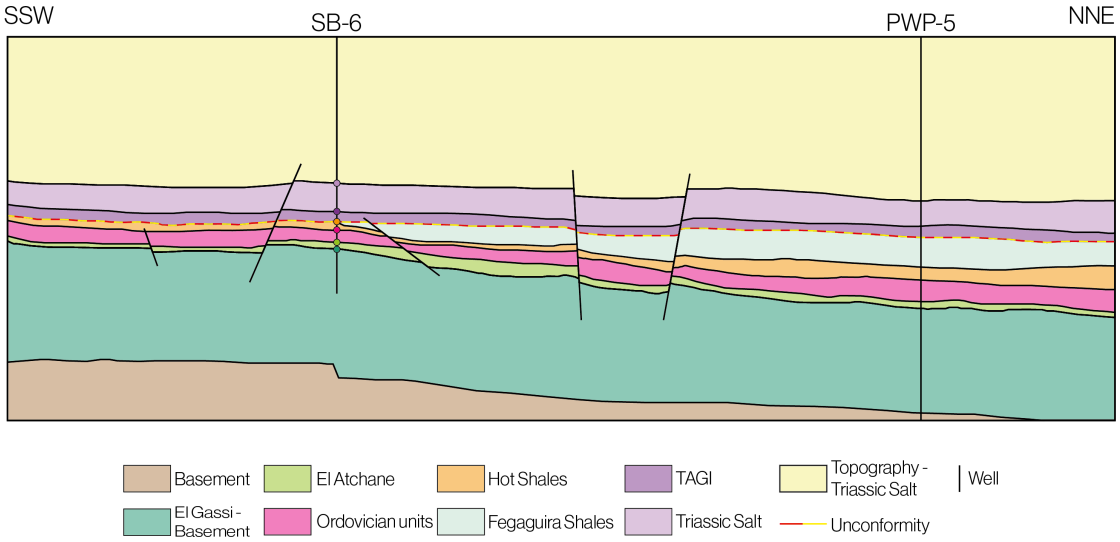

Figure 5.9: Interpreted sediment packages on previously depth converted seismic by Bruna et al. (2019a) used for migration modelling along NNE-SSW profile 5. Location in figure 3.5.

Scenario Validation

The low and high case migration models result in predicted present-day hydrocarbon accumulations (figures 5.10 & 5.11 respectively). Validation of the migration models is possible in well SB-6, which shows hydrocarbon discoveries in the Triassic TAGI and Ordovician El Atchane units. The high case model accurately simulates accumulations around this well, while the low case model shows no hydrocarbons close to well SB-6. Therefore, the high case model is deemed most representative for migration in the area of interest and the low case model is not considered in further interpretation. Additionally, migration simulations for the high case model along E – W oriented profile 1 emphasizes migration and reservoir charging varies spatially in the area of interest (figure 5.12).

Migration History

The basin experienced significant burial until the Late Permian (ca. 260 Ma) when the maximum Paleozoic burial depth is reached (figures 5.11 & 5.12). This period marked the onset of hydrocarbon generation in the Silurian – Early Devonian Fegaguira shales and Hot Shales. The thick package of Fegaguira shales has good sealing properties and overlie the Hot Shales, the superior source rock. High capillary entry pressure in the Fegaguira shales prevents upward migration and likely forced hydrocarbons to migrate downwards into the Ordovician and El Atchane units. There hydrocarbons migrate laterally to traps within these units, i. e. anticlines, faults. Lateral migration occurs less in E – W direction due to pre-existing faults (figure 5.12).

Once Hercynian exhumation concluded (ca. 250 Ma) there is no ongoing active generation in the area of interest (figures 5.11 & 5.12). The Fegaguira shales, Hot Shales and Ordovician units are brought up to the surface and (partially) eroded in the SSW and W. Further away from the Telemzane Arch, in the NNE and E, thick packages of Fegaguira and Hot Shales are preserved overlying the Ordovician units. These shales act as a seal,

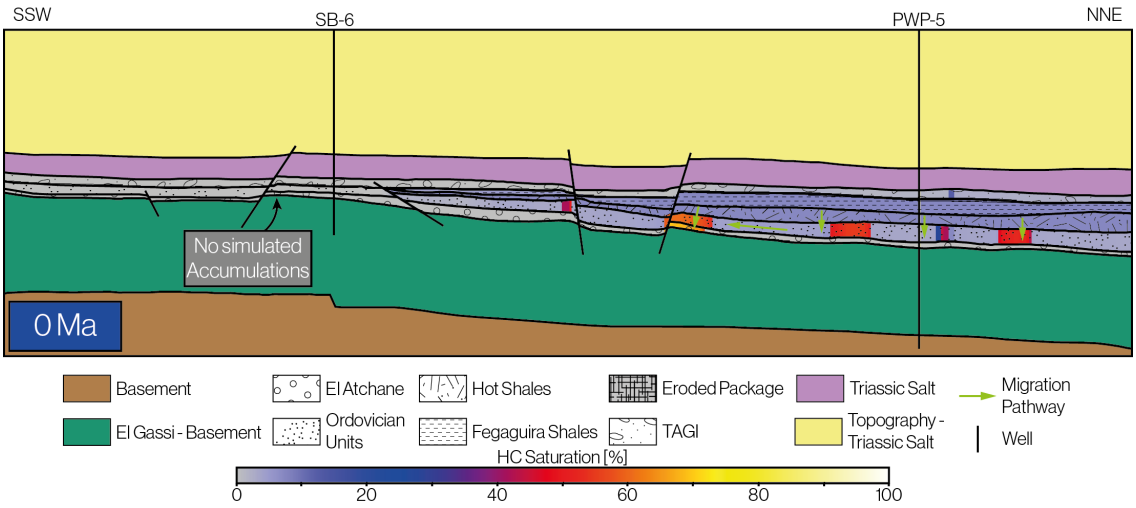

Figure 5.10: Hydrocarbon saturation distribution along a SSW – NNE profile (profile 5 in figure 3.5) at 0 Ma using the calibrated low case burial history. Hydrocarbon discoveries around well SB-6 are not simulated and therefore the calibrated low case burial history is deemed unrepresentative.

trapping and preserving the hydrocarbon accumulations in the Ordovician reservoirs. Within the Ordovician units hydrocarbons continues migrating laterally and mostly up-dip into traps. Some hydrocarbon also migrates further towards the SSW (figure 5.11). Here large amounts of hydrocarbon, generated prior to Hercynian exhumation, leaked to the surface.

After deposition of the TAGI and a regional seal (ca. 205 Ma), the Triassic salt, hydrocarbons accumulate in the TAGI unit (figure 5.11). Hydrocarbon previously trapped in the Ordovician units in the structural lows (NNE) migrated up-dip towards the SSW and along a fault into the TAGI- and El Atchane units (figure 5.11). Extension led to the formation of this fault, bringing the Ordovician units into contact with the TAGI- and El Atchane units. In E – W direction pre-existing faults prevent contact between the TAGI and Ordovician units. This prohibits extensive lateral migration, failing to charge the TAGI (figure 5.12). In the east minor amounts of preserved hydrocarbon migrate from the Fegaguira shales into the now overlying TAGI, but did not lead to major accumulations.

Extensive Mesozoic burial led to deposition of a thick sediment package resulting in the present-day situation (figure 5.11 & 5.12). Due to major maturation in the Paleozoic, only minor renewed hydrocarbon generation occurs in the preserved Fegaguira shales and Hot Shales. Expelled hydrocarbon migrates downward into the deeper lying Ordovician and El Atchane units in the NNE and E. Potential accumulations are hosted in structural traps in the Ordovician and El Atchane units, prevented from upwards migration by the overlying Hot Shales and Fegaguira shales. Hydrocarbon proceeds to migrate laterally from the NNE towards the SSW (figure 5.11). Around well SB-6 this charged the TAGI- and El Atchane units, validated by hydrocarbon discoveries in this well. Accumulations from the east do not reach the TAGI in well SB-6 and therefore this area does not contribute to the charging of this unit (figure 5.12).

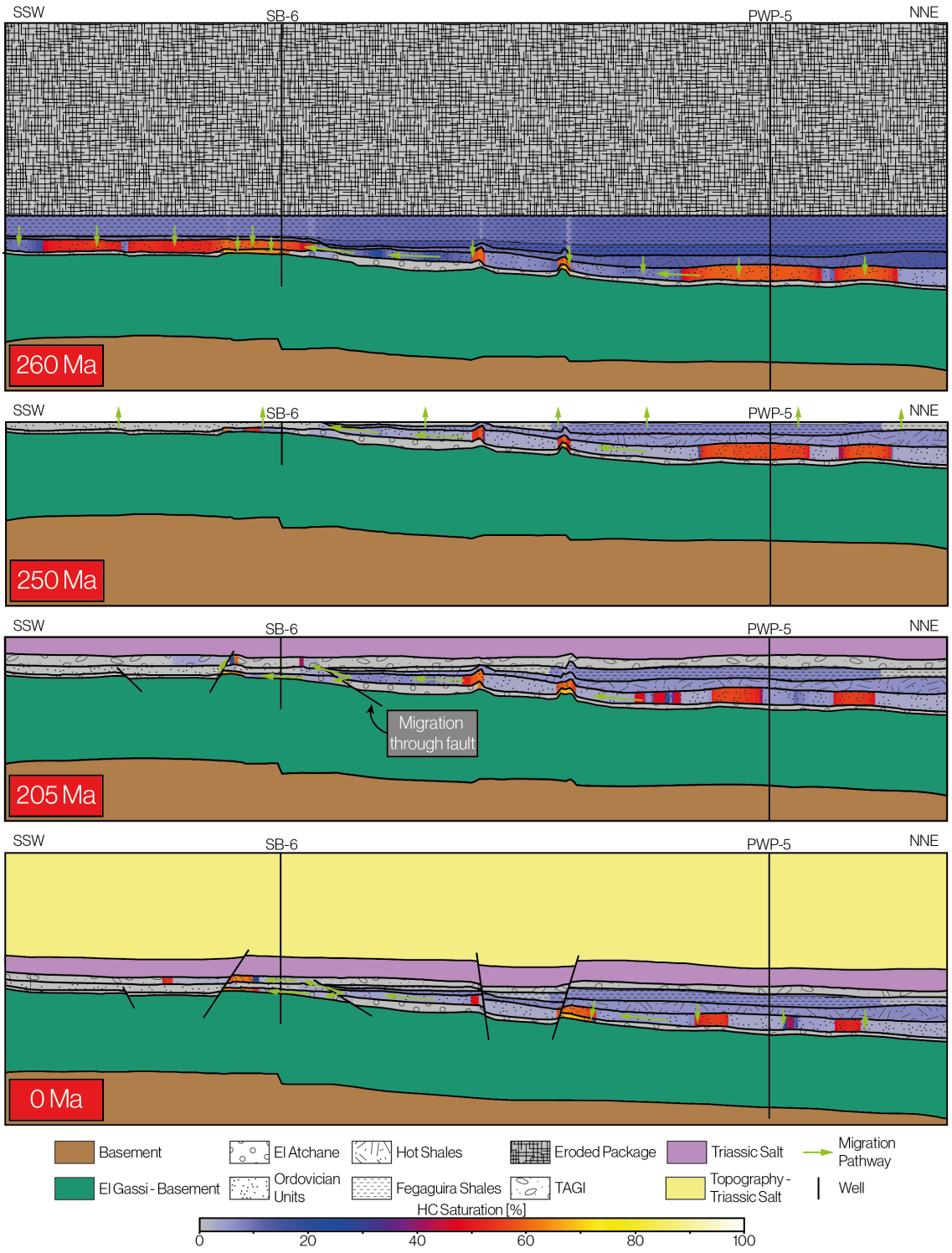

Figure 5.11: Simulated hydrocarbon saturation distribution along a SSW – NNE profile (profile 5 in figure 3.5) at 260, 250, 205 and 0 Ma using the calibrated high case burial history. Accumulations result from migration pathways simulation through time.

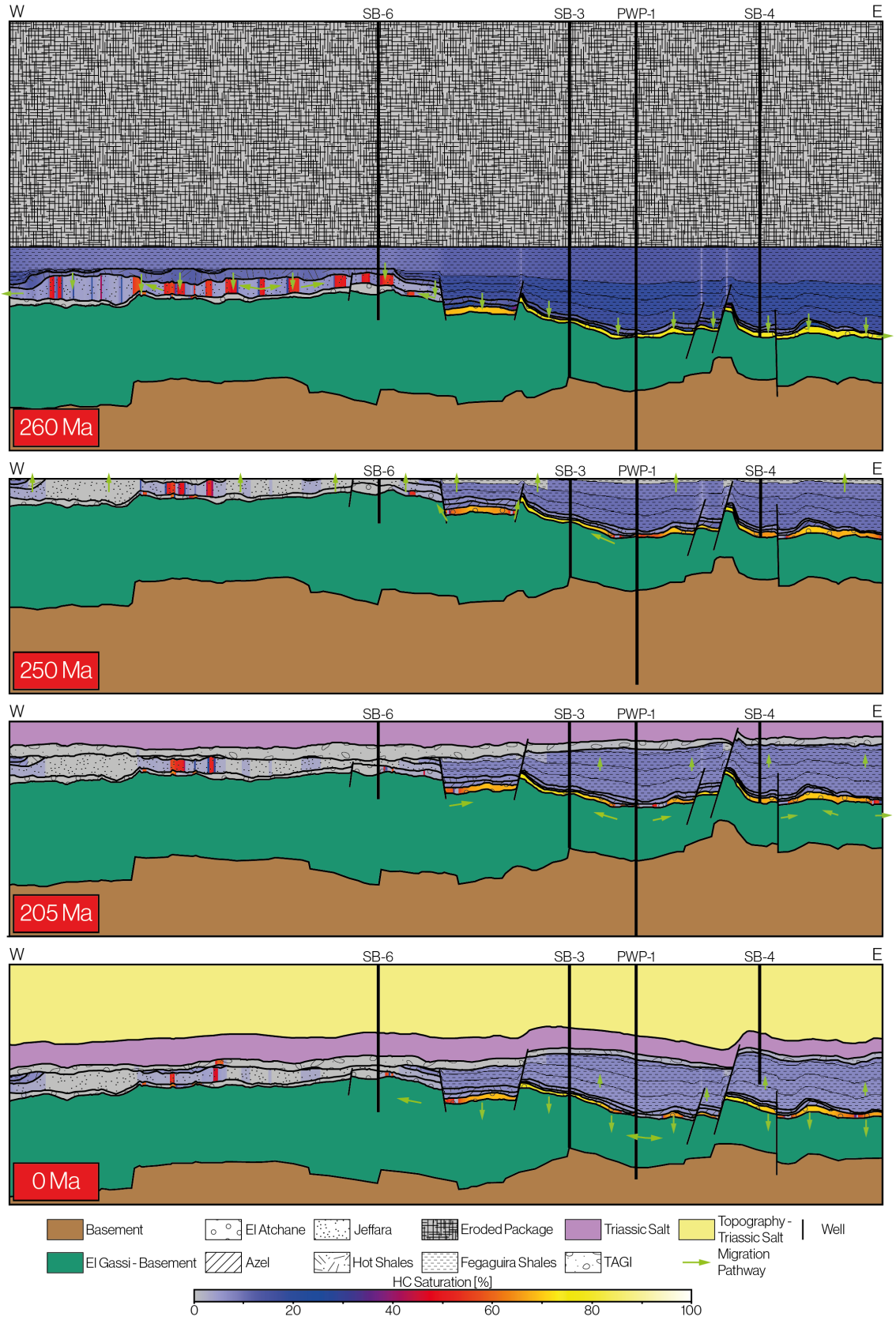

Figure 5.12: Simulated hydrocarbon saturation distribution along a E – W profile (profile 1 in figure 3.5) at 260, 250, 205 and 0 Ma using the calibrated high case burial history. Accumulations result from migration pathways simulation through time.

6 IMPLICATIONS ON PETROLEUM SYSTEMS

6.1 INTERPRETED PETROLEUM SYSTEMS

The simulated hydrocarbon accumulations in the migration study (figures 5.11 & 5.12) show accumulations that laterally terminate abruptly indicating lack of lateral resolution. Similarly, the sediment packages in the model lack vertical resolution, failing to capture the vertical distribution of hydrocarbons. This is caused by the limited number of cells describing a unit, which is minimized to reduce computational requirements. As a result, the simulated hydrocarbon accumulations indicate where hydrocarbons are trapped, but does not accurately represent effects of buoyancy between water and hydrocarbon. This resulted in patches of hydrocarbon located away from traps. In addition to this, the lithofacies distribution within the sediment packages is not considered at this stage. These limitations are considered in the interpretation and schematic depictions of the petroleum systems in the area of interest (figure 6.1). The migration study suggests the presence of at least 4 petroleum systems in the Southern Chotts Basin (figure 6.1).

1. "Triassic System" in the south of the area of interest sourced by the NNE.
2. "Central Ordovician System" in the center of the area of interest sourced through downward and lateral migration from multiple directions.
3. "N Deep Ordovician System" in the NNE, locally sourced by downward close proximity migration.
4. "E Deep Ordovician System" in the east, locally sourced by downward close proximity migration.

The TAGI unit of the Triassic System shows local high hydrocarbon saturation within the southern part of the area of interest, near well SB-6 (figure 6.1). The contacting Ordovician and TAGI units and impermeable Triassic salt unit are of high importance to this system, allowing lateral up-dip migration of preserved Paleozoic hydrocarbons and preventing upward migration. Simulation results indicated the TAGI unit is mainly sourced by Paleozoic generation in the NNE, while generation in the east does not contribute to the charging of this unit.

The El Atchane unit shows high hydrocarbon saturation around well SB-6 (figure 6.1). These accumulations in the Central Ordovician System are partially locally generated during the Paleozoic. Additional charge comes from preserved Paleozoic hydrocarbons in the NNE and east. Within the El Atchane unit they migrate laterally to structural traps and are prevented from upwards migration into the TAGI by a thin Fegaguira and Hot Shales package. As a result the hydrocarbons originating from various sources mix and form present-day accumulations.

In the northern part of the area of interest, the deeper lying Ordovician units and El Atchane show multiple hydrocarbon accumulations trapped underneath a thick package

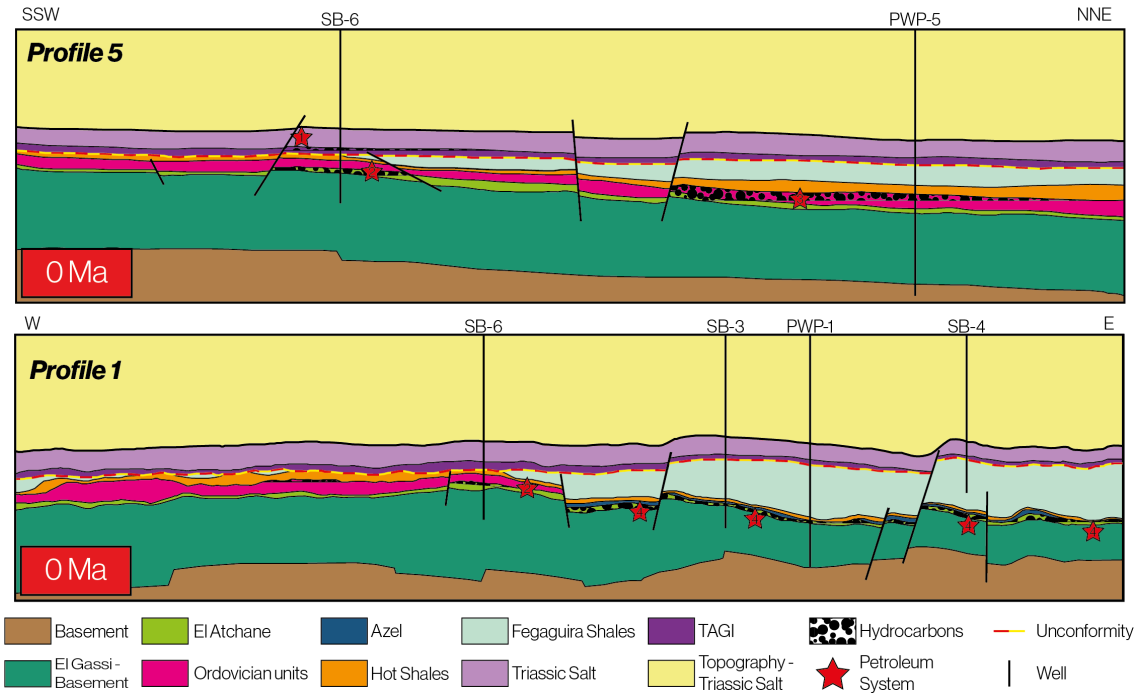

Figure 6.1: Schematic depiction of the 4 interpreted petroleum systems along the NNE – SSW profile 5 and E – W profile 1 in the area of interest (location in figure 3.5).

of Fegaguira and Hot Shales (figure 6.1). The migration study results shows that the majority of the hydrocarbons found in the Triassic and Shallow Ordovician Systems originate here. Hydrocarbons in this N Deep Ordovician System are locally generated during the Paleozoic and experienced minor additional charging during the Mesozoic. Subsequent lateral migration to local anticlines in the porous Ordovician units traps the hydrocarbons, where the overlying shales prevent upward migration.

The eastern part of area the El Atchane hosts multiple hydrocarbon accumulations in deeper lying faulted blocks, constituting the E Deep Ordovician System (figure 6.1). Paleozoic generation charged the El Atchane through downward migration, where hydrocarbons locally migrated to structural traps such as local anticlines or up-dip in the faulted blocks. The Azel, Fegaguira and Hot Shale units prevent upward migration. Minor amounts of renewed generation further charged the system during the Mesozoic.

6.2 LOCAL KITCHEN AREA

The identified petroleum systems are primarily sourced by Paleozoic maturation of the Silurian – Early Devonian Fegaguira and Hot Shales. Generated hydrocarbons migrated downwards into the underlying Ordovician and El Atchane units. High capillary entry pressures in the Fegaguira and Hot Shales prevented upwards migration and allowed subsequent lateral migration towards structural traps. These hydrocarbons preserved wherever thick packages of Fegaguira and Hot Shales are preserved during Hercynian exhumation (figure 6.1). Elsewhere, Hercynian exhumation caused hydrocarbon leakage.

The interpretation of the migration study results (figure 6.1) indicates that thick packages of Fegaguira and Hot Shales are generally preserved wherever present-day Hot Shale

depth exceeds 3750 m. This generally coincides with the NNE and E portion of the basin and suggests this further argues the importance of this area (figure 6.2). In the western portion of the area of interest these shales have not been well preserved during Hercynian exhumation (figure 6.1). Seismic data in the area of interest suggests that the Hot Shales extend at similar depths towards the N and NE. This indicates additional matured source rock may be found in these areas, possibly extending the petroleum kitchen area.

Figure 6.2: Extent of the petroleum kitchen, located in the NE portion of the area of interest. Kitchen area preserved significantly thick Fegaguira and Hot Shales such that hydrocarbon migrated downward into the Ordovician and El Atchane units. In the western portion of the area of interest these shales are only preserved in thin packages and resulted in hydrocarbon leaking.

Hydrocarbon discoveries in well SB-6 confirm the simulated hydrocarbon accumulations in the TAGI and El Atchane units are sourced from the NNE and east. Mohamed et al. (2014) conducted oil – source rock correlation between the Fegaguira and Hot Shales and oil samples from the Ordovician and Triassic. This confirms that Ordovician and Triassic reservoirs in the Southern Chotts basin are sourced by local Fegaguira and Hot Shales, as is also mentioned by Mejri et al. (2006) and Soua (2014b).

In addition to this, available geochemical fingerprint comparison of these discoveries shows similarities in their composition. However, due the present compositional differences it remains unclear if they share the same source location. The migration study showed the El Atchane unit near well SB-6 is primarily charged by the source rocks in the NNE, with minor contribution from the east. This resulted in mixing of hydrocarbon charge in the Ordovician reservoirs and may explain the compositional differences between the hydrocarbon discoveries in well SB-6. In any case, it suggests the NNE and eastern portion of the area of interest both contributed to reservoir charging in the remainder of the area and functioned as the petroleum kitchen (figure 6.2).

7 DISCUSSION

7.1 REGIONAL EXTENT KITCHEN AREA

Regional seismic data indicates that the Hot Shales are extensively deposited in the Southern Chotts Basin (figure 7.1). In the north and NE portion of the basin, these Hot Shales are currently buried deeper than in the area of interest, suggesting they experienced higher maturation. These areas are located further away from the Telemzane Arch and experienced less erosion of the source rock. Therefore, the north and NE likely host thicker and more mature packages of Fegaguira and Hot Shales than the area of interest. Towards the east, the Fegaguira and Hot Shales are currently buried at shallower depths, making it unlikely for hydrocarbon to migrate into the area of interest.

Figure 7.1: Potential extent of the regional kitchen area in the Southern Chotts Basin, as observed in seismic data (TWT). The north and NE portion of the basin shows significant potential of matured source rock. Potential migration pathways depict how matured source rock in the regional kitchen area may have reached the area of interest. Contribution of potential regional kitchen to reservoir charging in the area of interest is currently unknown.

Source rock maturation in the north and NE of the basin may have contributed to charging of hydrocarbon accumulations in the up-dip situated area of interest. Therefore, expelled hydrocarbon potentially migrated towards the area of interest. Our migration study suggested the petroleum kitchen in the area of interest primarily sourced accumulations in close proximity. Migration over larger distances up-dip resulted in hydrocarbon leaking during the Hercynian exhumation due to erosion of the seal.

When migrating over larger distances, the probability of hydrocarbon leakage becomes larger, due to e. g. faults, lithofacies heterogeneity, flow baffles. Matured source rock in closer proximity is more likely to contribute to reservoir charging in the up-dip situated

area of interest. As a consequence, the potential regional extent of the kitchen area is uncertain.

To resolve the uncertainty associated with regional migration distance, migration can be simulated along the NNE – SSW trending regional seismic sections (figure 7.1). This would require additional detailed seismic interpretation along the section, which is currently not possible due to a lack of well control. Such a study would provide insight in the extent of a potential regional petroleum kitchen and its contribution to reservoir charging in the area of interest.

7.2 FURTHER EXPLORATION

7.2.1 *Triassic System*

The migration study indicated only a single accumulation of hydrocarbons in the Triassic TAGI reservoir in well SB-6. The TAGI unit deposited in a N – NE directed fluvial channel belt (figure 7.2) and is characterised with lateral rapidly changing lithofacies and reservoir properties (Derguini et al., 2005). According to Derguini et al. (2005), the Net-to-Gross ratio increases eastwards, indicating the most promising reservoir parameters are located east of the area of interest. Well SB-4 penetrates the area marked by Derguini et al. (2005) to host these fluvial sands but showed a shaly TAGI unit, once again emphasizing the heterogeneity of fluvial deposits. Therefore, there is currently no constrain on the extent of the TAGI stacked sand deposits in the vicinity of the area of interest.

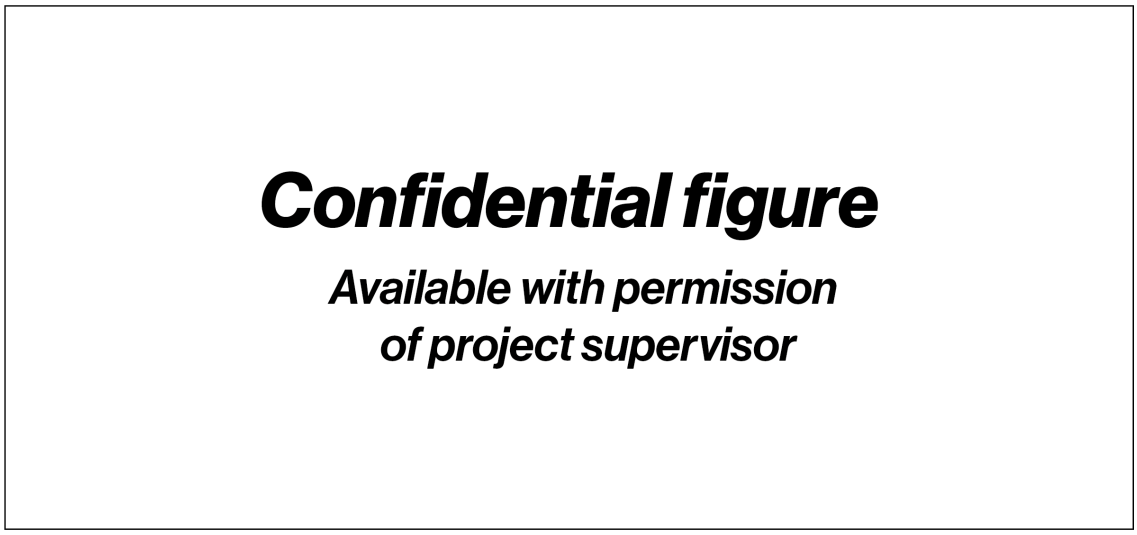

Figure 7.2: Schematic depiction of fluvial channel belt system the TAGI units. Main channel experienced avulsion over time. Net-to-Gross ratio increases eastwards, which is accompanied by better reservoir properties. **Note:** The channel dimensions are not to scale and solely schematically depict the depositional environment. Modified from Derguini et al. (2005).

The migration study does not simulate any significant hydrocarbon in well SB-4 sourced along the E-W section. However, simulations showed that the TAGI unit in well SB-6 is sourced by the NNE portion of area of interest. This suggests similar NNE sourcing of the TAGI unit may have occured eastward of the area of interest, where higher Net-to-Gross is predicted by Derguini et al. (2005). This area may host more stacked channel sand de-

posits, which is accompanied with better reservoir connectivity. A migration study along a seismic transect aligning roughly with the channel axis, east of the area of interest, can indicate whether these fluvial sands are charged similarly to well SB-6 (figure 7.2). However, with no well constraints available locating these stacked sands, evaluating the reservoir potential is not viable at this stage. It would be advised to resort to investigating the potential of the other petroleum systems.

7.2.2 *Ordovician Systems*

Multiple simulated present-day accumulations within the deeper lying Ordovician and El Atchane units indicate a vast potential of hydrocarbons is trapped underneath the Silurian – Early Devonian source rock in structural traps. The Central Ordovician system (well SB-6) also shows hydrocarbon trapping in similar deposits receiving petroleum charge from multiple directions. This makes these prospective systems suitable for further exploration. Previously, these structural lows, hosting the petroleum kitchen, were not yet identified as prospective reservoir opportunities. As a result no wells are available to constrain the potential of N and E Ordovician System.

The majority of the hydrocarbons in these systems originate in the Paleozoic, implying there is a probability they could be affected by degradation (Welte et al., 1997). However, the maturation study results showed the kitchen area source rock is currently in the condensate and wet-gas zone. Therefore, hydrocarbons trapped in the underlying Ordovician units likely did not experience thermal decomposition. In addition, the migration study results showed no signs of trap breaches. Therefore, it is likely that the simulated hydrocarbon accumulations were preserved.

The potential reservoir rocks for the Deep Ordovician system are the El Atchane and the Ordovician units, which contains the Hamra and the Jeffara packages. The El Atchane and Hamra units are deposited on a NW - SE striking siliciclastic shoreface (Derguini et al., 2005). This implies that the lithofacies, and therefore the reservoir potential, changes depending on the location within the shoreface environment. Confidential report estimated the lithofacies distribution of this shoreface system based on well data in the area of interest. Gharsalli and Bédir (2020) shows such a shoreface system extends eastward along the Telemzane Arch. The projection of this trend parallel to the Telemzane Arch indicates where to expect the best reservoir characteristics in the Ordovician systems (figure 7.3).

The lower shoreface lithofacies contain the best reservoir properties ($\phi_{avg} = 8\%, k_{avg} = 14$ mD) and are generally associated with the El Atchane unit (Derguini et al., 2005). The upper shoreface lithofacies mostly consists of highly cemented, but occasionally fractured, quartzarenite belonging to the Hamra formation. This makes the Hamra a tight reservoir associated with poor matrix properties ($\phi_{avg} = 8\%, k_{avg} = 1$ mD), which is locally improved by naturally occurring fractures (Derguini et al., 2005; Smith, 2020). The offshore facies contain negligible reservoir potential and are generally associated with the El Gassi marine shales (Gharsalli and Bédir, 2020). These shoreface deposits experienced local erosion due to deposition of the glacio-marine and deltaic deposits of the overlying Jeffara formation, but to what extent throughout the area of interest remains unclear. Considering this, the upper – lower and lower shoreface facies belts have the most potential to contain sweet spots in the Ordovician deposits.

The Deep Ordovician Systems concentrates in areas where thick packages of Fegaguira- and Hot Shales are preserved during the Hercynian exhumation. These matured shales

Figure 7.3: Schematic depiction of the siliciclastic ramp facies distribution within the area of interest, as modified from confidential report. The initial distribution is projected eastward parallel to the Telemzane Arch to estimate the distribution in the remainder of the area of interest. Lower shoreface facies of the El Atchane unit contain the best reservoir properties.

sourced the area and its surroundings, locally prevented upward migration and were crucial to the development of these systems. The interpretation of the migration study results indicated that thick packages of matured Fegaguira and Hot Shales are generally preserved wherever present-day Hot Shale depth exceeds 3750 m.

Figure 7.4: Extent of the Deep Ordovician system marked on Hot Shale Depth map. The Deep Ordovician System extends wherever thick packages Fegaguira Shales preserved during the Hercynian exhumation. The lithofacies distribution influences (figure 7.3) the reservoir potential within the system. The sweet spot area is marked by lower shoreface facies belt.

Within these areas the hydrocarbon migrated up-dip to local structural traps, e. g. tilted fault blocks, anticlines. This results in slim possibilities of hydrocarbon accumulations in the structural lows, exceeding depths of ca. 3950 m. Additionally, the lithofacies dis-

tribution of the shoreface deposits largely influences the reservoir potential. The lower shoreface lithofacies of the El Atchane show the best reservoir properties, marking the extent of the sweet spot area (figure 7.4). The upper shoreface facies associated with the Hamra are considered as a secondary target.

The sweet spot area marks an extent of ca. 37.25 km^2 in the deep Ordovician system. Currently, there is no well control on the thickness of the El Atchane in this sweet spot area. Therefore, we resort to an estimated El Atchane thickness of 25 – 50 m based on previous seismic interpretation for the migration study. To quantify the porous volume of the primary target, the sweet spot area is considered as a 37.25 km^2 by 25 – 50 volume of lower shoreface El Atchane sands. Considering the lower shoreface lithofacies' porosity averages 8%, the pore volume in the sweet spot area between 74,500,000 – 149,000,000 m^3, or 468.5 – 937 MM barrels.

Note that the thickness estimates are uncertain and therefore the computed volumes serve solely as an initial (likely optimistic) indication of the pore volume. The reservoir properties and lithofacies will vary throughout the sweet spot area and likely result in a lower pore volume. Furthermore, this study did not quantify the volumes of expulsed hydrocarbon, which should be further investigated in order to estimate in place volumes.

7.2.3 *Deep Ordovician Potential in Southern Chotts Basin*

The Deep Ordovician system is characterised by upper – lower shoreface siliciclastic deposits which are closely overlain by a thick package of impermeable shales. The organic rich "Hot Shale" member is situated at the bottom of the shales and is covered by a sufficiently thick package of less organic rich shales which is crucial for downward migration. This whole system should be sufficiently buried to mature the source rock and initiate hydrocarbon generation. However, if the system experienced excessive burial the source rock may become over mature and the hydrocarbon may have experienced thermal degradation. In addition to this, the siliciclastics may have experienced excessive cementation and lost its reservoir potential.

The high capillary entry pressure of the impermeable lower quality shales covering the hot shales will force hydrocarbons down into the porous units. Hydrocarbon migrates into local structural traps, e. g. anticline and faults, and are trapped by the source rock. Preservation of the overlying shales during exhumation is crucial to prevent hydrocarbon leaking. During reburial no significant trap breaching can occur.

The two most important features that can be investigated to predict the possible occurrence of a petroleum system similar to the Deep Ordovician system are 1) Extent of the siliciclastic ramp, and 2) Preservation of the Fegaguira and Hot Shales. Further eastward projection of shoreface system, parallel to the Telemzane Arch as implied by Gharsalli and Bédir (2020), marks the extent of potentially similar shoreface deposits. Most of region is expected to contain predominantly offshore lithofacies and is therefore unlikely to offer reservoir potential. Regional seismic transects provide insight in the extent of source rock erosion towards the east. If the Fegaguira and Hot Shales is absent there is no potential for a similar petroleum system. Eliminating these areas with no potential leaves a belt that has a possibility to hold a similar petroleum system as the Deep Ordovician System (figure 7.5).

Note that there is no well control on the shoreface deposits as none of the available eastward located wells penetrate the Ordovician sequence. Additionally, the Paleozoic

Figure 7.5: Evaluation of Deep Ordovician occurrence on a regional scale by process of elimination. Remaining area may contain the correct combination of shoreface deposits with reservoir potential and preservation of Fegaguira and Hot Shales. **Note:** Further investigation of this area is required to judge its potential.

deposits are buried more shallow towards the east, suggesting this area experienced a different burial history. How this precisely affected the petroleum system needs to be further investigated, but it potentially led to a different maturation history. Therefore, the remaining potential area merely marks where the right combination of shoreface deposits and preserved source rock may occur. Most importantly, the eliminated area marks the extent of where not to expect the Deep Ordovician petroleum system. Considering the up-dip location with respect to the potential regional kitchen area (figure 7.1), the projected lower shoreface belt offers a good prospect. However, further investigation of, e. g. presence of traps, source rock maturation, hydrocarbon migration, lithofacies distribution, and trap breaching, is required to judge its potential.

7.3 LATE CARBONIFEROUS – EARLY PERMIAN EXHUMATION PHASE

Soua (2014b) shows the Silurian – Early Devonian shales are locally overlain by Permian – Triassic deposits in the Southern Chotts basin. We previously debated the possibility of Permian deposits extending through the northern portion of the area of interest. However, the lack of well control on the undefined Paleozoic deposits in the area of interest resulted in disposing this possibility. However, since well data (well RG-6) in close proximity of the schematic seismic east of the area of interest shows Permian sand deposits, the impact of this possibility on the tectonic history is investigated (figure 7.6).

Permian deposits overlying the Silurian – Early Devonian indicates a major time gap that can not be explained by a single exhumation phase at the Late Permian – Early Triassic. This is supported by seismic interpretation, showing internal reflectors within the Permian and underlying formations are truncated at different angles by the "Hercynian" unconformity. Such a wedge shape suggests multiple stages of erosion, which has locally resulted in stacking of the unconformities as suggested by Frizon de Lamotte et al. (2013).

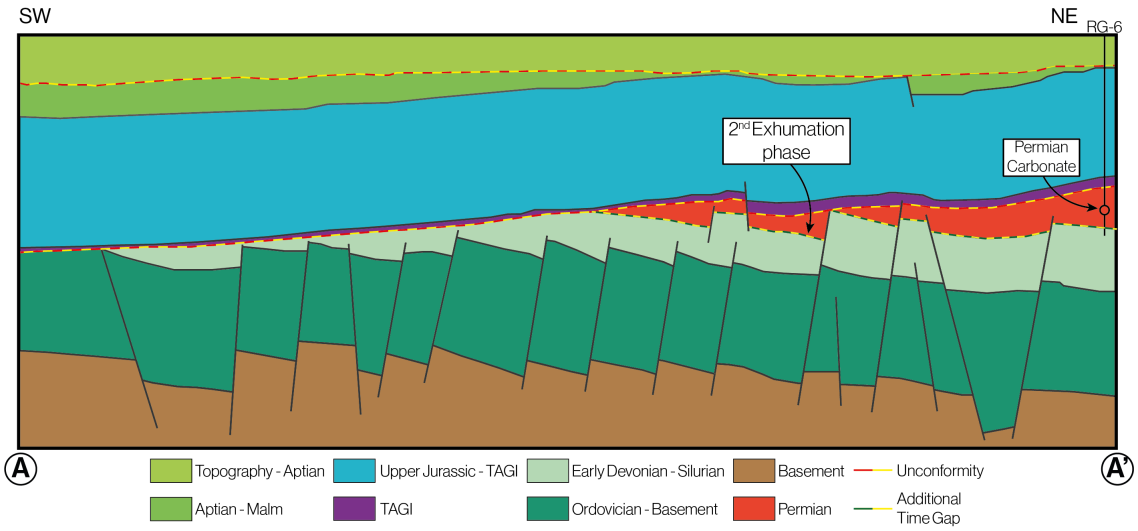

Figure 7.6: Schematic depiction of the present-day structure within the Southern Chotts Basin, east of the area of interest (location in figure 2.1). Revision of additional well data in close proximity of the seismic transect indicates that Permian deposits directly overlie Silurian – Early Devonian deposits.

Therefore an additional exhumation phase is required, occurring as late as the Carboniferous – Permian transition (ca. 290 Ma).

Despite the absence of the Permian in the area of interest, and therefore the absence of direct proof exhumation occured at the Carboniferous – Permian transition, the close proximity of the contact between Silurian – Early Devonian and Permian packages gives reason to investigate the effects of such a burial history scenario on the source rock maturation. "Double phase Hercynian" burial histories are constructed, maintaining the same assumptions as for the "single phase Hercynian" burial histories apart from the single phase Hercynian exhumation (figure 7.7). The maximum Paleozoic burial depth is reached by the end of the Carboniferous, whereafter the complete Early Devonian – Carboniferous series eroded. The Permian is deposited and thereafter eroded during an exhumation phase at the Late Permian – Early Triassic.

The previously selected heat flow model results in accurate estimation of the VR and VRE data for both double phase burial histories. Calibration of the Paleozoic burial depth previously indicated Hercynian exhumation does not exceed 2300 m of eroded sediment (figure 5.2), which is in line with the double phase Hercynian burial histories. The resulting VR and TR profiles in the kitchen area (PWP-5) indicate that the source rock maturation at present-day remains unaffected (figure 7.8). Independent of the amount of "Hercynian" phases, the source rock experiences its deepest burial depth at present-day. Thermal maturation depends on a combination of temperature and time spend at that temperature (Peters and Cassa, 1994). Therefore the present-day burial depth resulted in the maximum maturation.

The additional Hercynian exhumation phase primarily affects the timing of maturation and generation. Initial hydrocarbon generation starts earlier when considering the double phase high case (figure 7.8). However, Paleozoic hydrocarbon generation terminates with the start of the Early Hercynian phase in the Late Carboniferous. This results in slightly lower TR for the double phase scenario when comparing the high cases. While reaching

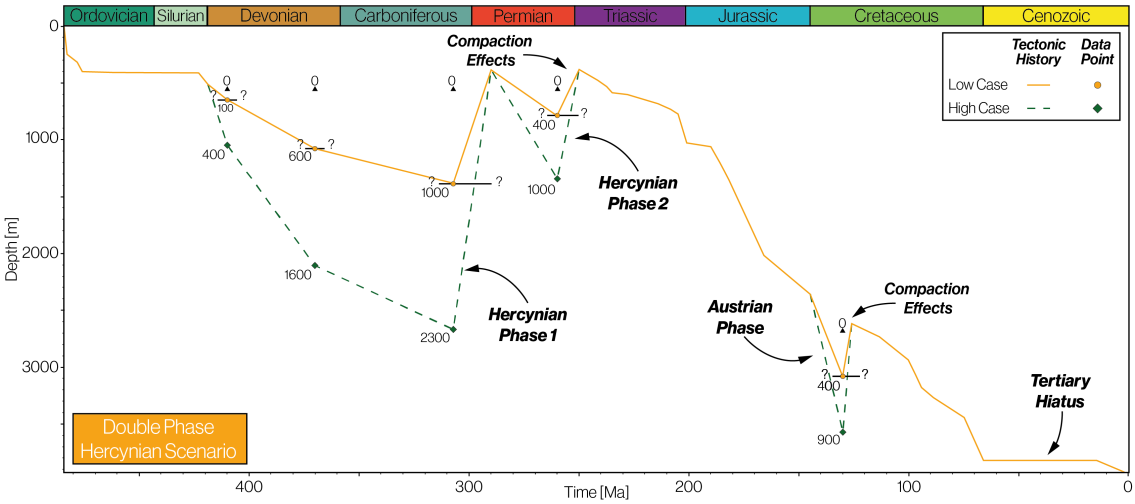

Figure 7.7: Burial history scenarios regarding a double phase Hercynian exhumation at the Carboniferous – Permian transition and the Late Permian – Early Triassic respectively. All other assumptions remain the same. Eroded sediments are initially deposited under equi-thickness conditions in the area of interest. Null case assumes no erosion and therefore experiences less compaction.

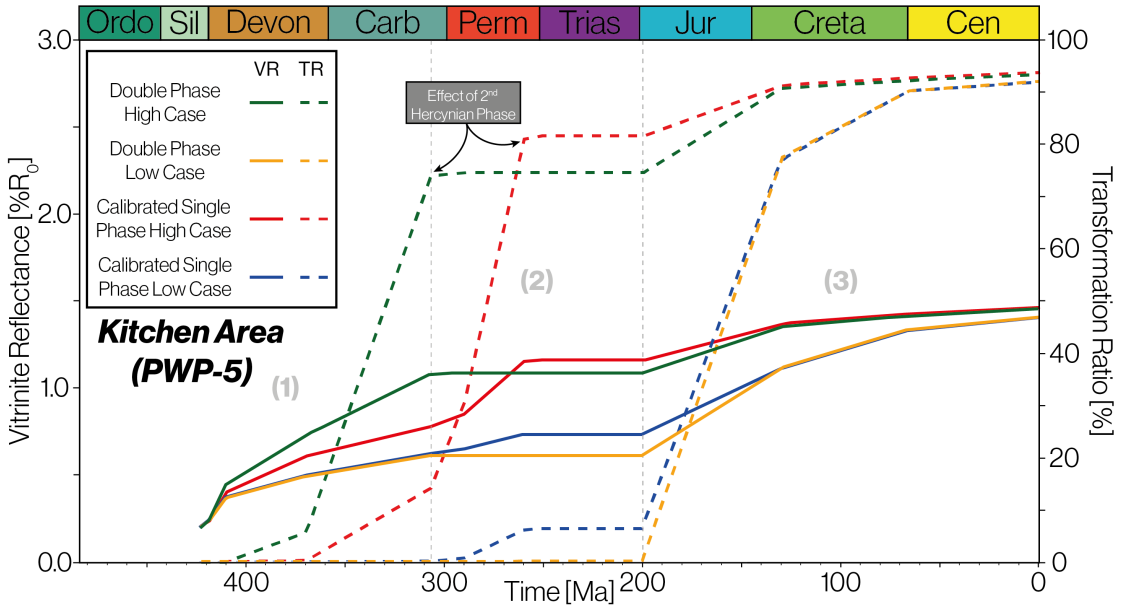

Figure 7.8: Hot Shale maturation history in kitchen area (PWP-5) for the double phase and calibrated single phase burial histories. Timing of maturation is primarily affected by addition of an Hercynian exhumation phase. Amount of Paleozoic maturation decreased as timing of maximum Paleozoic burial now coincides with lower heat flow.

the same maximum burial depth, but at different times, lower Carboniferous heat flow (figure 5.4) causes the decrease in Paleozoic TR. As Paleozoic hydrocarbon generation decreased, this potential is transferred to the Mesozoic. According to our initial sediment deposition estimates the Late Hercynian phase did not exceed the previous maximum burial depth. This results in an extended period of stable maturation for the double phase scenario when comparing the high cases (figure 7.8).

7.4 LIMITATIONS & RECOMMENDATIONS

7.4.1 *Burial History and Heat Flow Model*

Considering the limited available dataset, the proposed burial and heat flow model offer a representative history of the area. This served as adequate input to investigate source rock maturation and hydrocarbon migration within the area of interest. In addition to this, the timing of important extension and compression phases during the Late Paleozoic is still debated Frizon de Lamotte et al. (2013) and Galeazzi et al. (2010), with a new interpretation by Smith (2020) further pushing the discussion. Therefore, the proposed burial history and heat flow models should be calibrated with Low Temperature Thermochronology (LTT) obtained from rock samples containing apatite and/or zircon crystals. LTT methods, e. g. Apatite and Zircon Fission Track (AFT and ZFT) and Apatite-He and Zircon-He dating, provide information on the thermal history of the basin and help decipher the age at which crystal cooling initiated. As rocks generally cool with exhumation this allows to estimate the age of an exhumation phase (Peyton and Carrapa, 2013).

Each LTT technique has a specific temperature window over which it provides information. When applying multiple techniques to the same sample, the amount of exhumation experienced by the sample can be estimated (Peyton and Carrapa, 2013; Reiners and Brandon, 2006). The principles of these different LTT techniques are beyond the scope of this thesis and are described by Peyton and Carrapa (2013) and Reiners and Brandon (2006). LTT would improve calibration of exhumation timing and associated amount of erosion and therefore reduce the uncertainties in the basin history.

Subsidence analysis showed that all wells in the area of interest experienced similar subsidence patterns since the Mesozoic. Therefore, we assumed the evolution of the area can be represented by a common burial and thermal history for simplicity. Accurate calibration and validation of these models ensured their reliability for subsequent maturation- and migration studies. However, when applying this approach over a larger area, one common burial history will likely not suffice. Underdown et al. (2007) estimated the amount of exhumation in the Ghadames basin using sonic velocity, LTT and VR data from wells. The resulting areal distribution of exhumation defined region specific burial histories used in subsequent source rock maturation modelling. Subdividing the research area into regions based on areal distribution of exhumation would improve the accuracy of predicted maturation distribution.

7.4.2 *Source Rock Kinetics*

In the absence of source rock kinetics data Abu-Ali et al. (1999) offered a valid alternative to describe kerogen thermal decomposition. The modelled results provided useful insights in the petroleum systems within the area and accurately simulated hydrocarbon discoveries. However, selection of kinetics guides the modelled source rock maturation and hydrocarbon migration (Bora and Dubey, 2015). In addition, kerogen type and kinetic response are not systematically linked (Peters et al., 2006). Obtaining additional geochemical data to construct an area specific custom kinetics model will therefore result in more accurate simulation of source rock maturation. This will improve simulation of hydrocarbon migration, composition and volumes, which can be compared with avail-

able fluid inclusion data to give information on their spatial and compositional relation (Munz, 2001). Since the newly identified Deep Ordovician system is located underneath the petroleum kitchen, further exploration and geochemical data collection can be combined.

7.4.3 *Migration Study*

The migration study restores the seismic sections by sequentially removing overlying packages of sediments and decompacting the remaining units. However, deformational features along the section are not fully restored to their paleo-geometry. The source, reservoir and seal in the kitchen area are relatively undeformed allowing simulation of migration with simplified restorations. In addition, the migration study aimed to investigate local maturation and subsequent migration within the area of interest. The simplified restorations do not affect the amount of eroded sediment and thus the modelled source rock maturation. Despite the fact that a full restoration through time would result in a more realistic paleo-geometries, the insights provided by the migration study remain valid for petroleum system identification.

Migration modelled along 2D seismic transects and indicates several prospective traps and accumulations. In reality hydrocarbon migration and entrapment are 3D phenomenons, which should be considered when analyzing 2D sections (Bora and Dubey, 2015; Mann et al., 1997; Underdown and Redfern, 2008). Therefore the simulated accumulations are strictly hypothetical and do not necessarily represent mapped traps. However, the 2D sections are oriented such that they span the area of interest and capture its 3D geological complexity. This improved the understanding of reservoir charging in multiple directions and allowed to comprehend the areal distribution of the interpreted petroleum systems.

Due to differences in hydrocarbon composition discovered in the El Atchane and TAGI units in well SB-6, some uncertainties arise related to source location. The migration study suggested that the El Atchane discovery is sourced from multiple directions. Additional data on hydrocarbon discoveries in other wells would further improve the validation of simulated migration and helps decipher the relation between hydrocarbons discovered throughout the basin.

7.5 FUTURE RESEARCH

The Deep Ordovician system can be further explored with seismic attributes extracted from the 3D seismic block before targeting the system with an exploration well. In combination with available well logs, seismic attributes may help identify and map important reservoir parameters, e. g. porosity and fluid content (Chopra and Marfurt, 2007). This will help characterize reservoir heterogeneities and improve future well placement for further exploration of this system.

In addition to this, ongoing research conducted by Smith (2020) used seismic attributes to show the Ordovician reservoir units in the area of interest host well connected fractures. Whether these enhanced flow or not is yet to be determined by means of well testing. Smith (2020) mentions these fractures likely formed during the final stages of Hercynian exhumation. Therefore their presence may have favoured migration in a certain direction. The Discrete Fracture Network (DFN) models proposed by Smith (2020) could be imple-

mented in the lithofacies model of the Ordovician units. Subsequent statistically populating the Ordovician and TAGI units with the DFN model and lithofacies distributions will give insight in the effects on the hydrocarbon migration in the area.

Although costly, targeting local traps within the Deep Ordovician Systems with an exploration well has significant potential of hydrocarbon discoveries. Penetrating this sequence also provides the opportunity to obtain additional geochemical data on the Silurian – Early Devonian source rocks in the kitchen area. This would allow to develop laboratory calibrated source rock kinetics, as suggested by Peters et al. (2006), and improve our understanding of the kerogen thermal decomposition in Fegaguira and Hot Shales.

While the lithofacies of the distinguished units in the present-day stratigraphic column are considered in the migration study, their lateral distribution is not. This is especially important in reservoir units and carrier beds, as these impact the migration pathways and accumulations. E. g. the fluvial TAGI unit shows rapidly changing reservoir characteristics, for which connectivity and the resulting traps may vary from the modelled results. The El Atchane reservoir properties change laterally perpendicular to the shoreface with the changing lithofacies. This may favour hydrocarbon migration within the lower shoreface lithofacies belt and potentially migrate hydrocarbons away from traps. Further investigation on the distribution of these reservoir units, especially the El Atchane unit, helps constructing a more accurate estimate of the reservoir potential of the Deep Ordovician System.

Previously, we submitted a proposal to sample permeability and porosity in the Permian deposits found in the Tebaga de Medenine (appendix c). A similar approach can be taken for other outcropping deposits in the region, e. g. Triassic deposits. We proposed to do this by means of TinyPerm III handheld air permeameter measurements and laboratory liquid permeability measurements. In addition to this, a select amount of samples would be tested for permeability under high confining pressure, mimicking the setting in the subsurface. These measurements would allow to find a relation between permeability and porosity under surface and subsurface conditions. This relation translates the surface measurements and their spatial distribution to a subsurface setting, allowing for easier characterisation of large extents of potential reservoir rock. Subsequent population of reservoir units in the subsurface would allow to better estimate the lithofacies distribution within the surface. The relation between the samples extracted at the surface and the deposits in the subsurface are verified by analysing thin sections to determine whether these deposits have a similar diagenetic history.

Building further on the 2D migration study, there are possibilities to incorporate this into a 3D petroleum system model. Seismic data and interpretation are available for the construction of a 3D model. With a similar reconstruction through time migration can be simulated simultaneously throughout the entire area of interest. This would further improve understanding of hydrocarbon mixing from different areas of matured source rock.

8 CONCLUSION

In this thesis seismic and well data is used to construct and calibrate the basins tectonic and thermal evolution. Subsequent source rock thermal maturation modelling showed how the proposed basin evolution affects the maturation and generation histories. Migration simulations through time along multiple 2D transects allowed the investigation of potential petroleum systems within the basin. This allowed the following research questions to be answered:

1. **What is the tectonic and thermal evolution of the area of interest?**
   Seismic interpretation and well data showed the area of interest experienced 2 exhumation phases, Hercynian (ca. 260 – 250 Ma) and Austrian (ca 130 – 126 Ma), and a hiatus in the Tertiary (ca. 66 – 20 Ma). We focused on the Hercynian unconformity as it represents the largest time gap. Seismic data and adjacent analogue basins, with similar influence from the Telemzane Arch, allowed estimation of the amount of eroded sediment associated with exhumation. The tectonic and thermal history incorporated these phases.

   Minimizing the uncertainties in the proposed tectonic and thermal histories is achieved with vitrinite reflectance (equivalent) data calibration. Subsidence analysis indicated the area of interest experienced a similar subsidence history. Therefore the VR calibrated models accurately represent the tectonic and thermal history of the area of interest in subsequent thermal maturation modelling. Tectonic calibration indicated Paleozoic burial did not exceed 2300 m. Simulated hydrocarbon discoveries within the area of interest favour the calibrated high case burial history.

2. **How do exhumation phases affect the source rock maturation history?**
   Testing several tectonic histories with high and low estimates of erosion indicates that exhumation causes maturation in the Fegaguira and Hot Shales to occur in 3 distinct phases; i. e. (1) Paleozoic initial maturation, (2) Post-Hercynian stable maturation, and (3) renewed Mesozoic maturation. Paleozoic burial depth estimates primarily influence the timing of stage 2 and 3 and determines the level of maturation in the Paleozoic. This affects the generation zone the source rock is in at the end of the Paleozoic and start of the Mesozoic.

   In absence of wells penetrating the structural lows in the area of interest pseudo wells are crucial to model source rock maturation. Maturation modelling shows that the source rock in the kitchen area is currently in the condensate – wet gas zone.

   Review of additional well data in close proximity suggests the presence of an additional exhumation phase at the Carboniferous – Permian transition. In terms of source rock maturation this primarily affected the timing of the maturation phases, as the VR calibrated maximum Paleozoic burial depth remains unchanged. As a result, with unchanged thermal history, this also affects the maturation levels through time. The uncertainties related to the timing of exhumation can be further constrained with low temperature thermochronology.

3. **How does hydrocarbon migrate from source to present-day accumulations?**
   Investigation of migration through time suggests present-day hydrocarbon discoveries in well SB-6 are primarily sourced by Paleozoic generation in the kitchen area (well PWP-5). High capillary entry pressures forced hydrocarbons generated in Fegaguira and Hot Shales to migrate downward into porous Ordovician units. Wherever thick packages of these shales were preserved during Hercynian exhumation the hydrocarbons were prevented from leaking to the surface. These hydrocarbons migrated laterally up-dip and along faults to source the TAGI and El Atchane units. Migration study results indicate the hydrocarbons in El Atchane are sourced from multiple locations, which is supported by geochemical fingerprint analysis.

4. **What are the implications of the proposed basin history on the petroleum systems within the basin?**
   The migration study indicates the area of interest hosts at least 4 different petroleum systems, which are all sourced by Silurian – Early Devonian Fegaguira and Hot Shales. The accumulations in the Triassic and Central Ordovician Systems are validated with well SB-6. In these systems the Ordovician units act as carrier beds for lateral up-dip migration into structural traps. The Deep Ordovician Systems hosts accumulations in structural traps within Ordovician and El Atchane units. These systems situate in the central to NE portion of the area of interest, where they are overlain by thick packages of impermeable Fegaguira and Hot Shales preventing upward migration.

   Migration modelling showed that the present-day accumulations are primarily sourced from the NNE and E portion of the area of interest, which functions as the kitchen area. Seismic data suggests that the Hot Shales extend at increased depths towards the N and NE. This indicates additional matured source rock may be found in these areas and offers further prospects for investigation.

   The majority of the hydrocarbon generation in the area of interest occurs in the Paleozoic, implying these hydrocarbons have preserved over large times. Maturation modeling indicates the kitchen area source rock is in the condensate and wet-gas zone, indicating hydrocarbons trapped in underlying formations are unlikely to have experienced thermal decomposition.

5. **What could be potential exploration targets within the area of interest?**
   Structural traps, e. g. tilted fault blocks, anticlines, within the Ordovician and El Atchane units of the Deep Ordovician Systems offer the most potential for further exploration. The lower shoreface lithofacies of the El Atchane unit show the best reservoir properties ($\phi_{avg} = 8\%$ and $k_{avg} = 14$ mD) and is considered as the primary target of the Deep Ordovician System. This siliciclastic ramp system is directed towards the NE and laterally bounds the El Atchane with cemented upper shoreface (Hamra) and offshore (El Gassi) facies.

   Projection of the shoreface system along the Telemzane Arch marks the extent of the El Atchane unit within the area of interest. In order to trap hydrocarbons, these lower shoreface deposits should be covered with thick packages of preserved Fegaguira and Hot Shales. Mapping the simulated accumulations within this area marks the potential sweet spot area. Up-dip hydrocarbon migration makes structural highs within this are the most likely to contain hydrocarbon. On regional scale

the area where the Deep Ordovician System potentially occurs is marked through process of elimination. This area requires further investigation on e. g. trap presence, source rock maturation, and lithofacies distribution.

BIBLIOGRAPHY

Abu-Ali, Mahdi A., Jean-Luc L. Rudkiewicz, Jim G. McGillivray, and Françoise Behar (1999). "Paleozoic Petroleum System of Central Saudi Arabia." In: *GeoArabia* 4.3. _eprint: https://pubs.geoscienceworld.org/geoarabia/article-pdf/4/3/321/4553115/abuali.pdf, pp. 321–336. ISSN: 1025-6059.

Allen, P. A. and John R. Allen (2013). *Basin analysis: principles and application to petroleum play assessment*. Third edition. Chichester, West Susex, UK: Wiley-Blackwell. 619 pp. ISBN: 978-0-470-67376-8 978-0-470-67377-5 978-1-118-45030-7.

Bishop, William F. (1975). "Geology of Tunisia and Adjacent Parts of Algeria and Libya." In: *AAPG Bulletin* 59. ISSN: 0149-1423. DOI: 10.1306/83D91CA4-16C7-11D7-8645000102C1865D. URL: http://search.datapages.com/data/doi/10.1306/83D91CA4-16C7-11D7-8645000102C1865D (visited on 03/18/2020).

Bodin, S., L. Petitpierre, J. Wood, I. Elkanouni, and J. Redfern (Oct. 2010). "Timing of early to mid-cretaceous tectonic phases along North Africa: New insights from the Jeffara escarpment (Libya–Tunisia)." In: *Journal of African Earth Sciences* 58.3, pp. 489–506. ISSN: 1464343X. DOI: 10.1016/j.jafrearsci.2010.04.010. URL: https://linkinghub.elsevier.com/retrieve/pii/S1464343X10000920 (visited on 03/26/2020).

Boote, David R. D., Daniel D. Clark-Lowes, and Marc W. Traut (1998). "Palaeozoic petroleum systems of North Africa." In: *Geological Society, London, Special Publications* 132.1, pp. 7–68. ISSN: 0305-8719, 2041-4927. DOI: 10.1144/GSL.SP.1998.132.01.02. URL: http://sp.lyellcollection.org/lookup/doi/10.1144/GSL.SP.1998.132.01.02 (visited on 03/17/2020).

Bora, Deepender and Siddharth Dubey (Dec. 2015). "New insight on petroleum system modeling of Ghadames basin, Libya." In: *Journal of African Earth Sciences* 112, pp. 111–128. ISSN: 1464343X. DOI: 10.1016/j.jafrearsci.2015.08.020. URL: https://linkinghub.elsevier.com/retrieve/pii/S1464343X15300534 (visited on 04/07/2020).

Bouaziz, Samir, Eric Barrier, Mohamed Soussi, Mohamed M. Turki, and Hédi Zouari (Nov. 2002). "Tectonic evolution of the northern African margin in Tunisia from paleostress data and sedimentary record." In: *Tectonophysics* 357.1, pp. 227–253. ISSN: 00401951. DOI: 10.1016/S0040-1951(02)00370-0. URL: https://linkinghub.elsevier.com/retrieve/pii/S0040195102003700 (visited on 12/19/2019).

Bruna, Pierre-Olivier, Giovanni Bertotti, Salma Ben Amor, Ahmed Nasri, and Sondes Ouahchi (Oct. 2019a). "Analysis of the pre- and post Variscan unconformity deformations: new insights for the characterisation of the Ordovician and Triassic reservoirs in the Southern Chotts Basin, Tunisia." In: p. 4.

Bruna, Pierre-Olivier, Giovanni Bertotti, Salma Ben Amor, Ahmed Nasri, and Sondes Ouahchi (Nov. 25, 2019b). "Vertical movements and petroleum system modelling in the Southern Chotts Basin, Central Tunisia." In:

Chopra, Satinder and Kurt J. Marfurt (Jan. 2007). *Seismic Attributes for Prospect Identification and Reservoir Characterization*. Society of Exploration Geophysicists, European Association of Geoscientists, and Engineers. ISBN: 978-1-56080-141-2 978-1-56080-190-0. DOI: 10.1190/1.9781560801900. URL: https://library.seg.org/doi/book/10.1190/1.9781560801900 (visited on 10/02/2020).

Derguini, K., A. Tadjine, L. Fourati, Z. Day, A. Chabane, A. Gueham, and F. Omri (Mar. 2005). "Hydrocarbon Potential of Maatoug Permit." In: p. 174.

Dutton, Shirley P and Brian J Willis (Sept. 1998). "Comparison of outcrop and subsurface sandstone permeability distribution, Lower Cretaceous Fall River Formation, South Dakota and Wyoming." In: *Journal of Sedimentary Research* 68.5, p. 11.

Ehrenberg, S.N., G.P. Eberli, M. Keramati, and S.A. Moallemi (Jan. 2006). "Porosity-permeability relationships in interlayered limestone-dolostone reservoirs." In: *AAPG Bulletin* 90.1, pp. 91–114. ISSN: 0149-1423. DOI: 10.1306/08100505087. URL: http://search.datapages.com/data/doi/10.1306/08100505087 (visited on 01/30/2020).

Frizon de Lamotte, Dominique, Saeid Tavakoli-Shirazi, Pascale Leturmy, Olivier Averbuch, Nicolas Mouchot, Camille Raulin, François Leparmentier, Christian Blanpied, and Jean-Claude Ringenbach (Mar. 2013). "Evidence for Late Devonian vertical movements and extensional deformation in northern Africa and Arabia: Integration in the geodynamics of the Devonian world: DEVONIAN EVOLUTION NORTHERN GONDWANA." In: *Tectonics* 32.2, pp. 107–122. ISSN: 02787407. DOI: 10.1002/tect.20007. URL: http://doi.wiley.com/10.1002/tect.20007 (visited on 03/20/2020).

Galeazzi, S., O. Point, N. Haddadi, J. Mather, and D. Druesne (Jan. 2010). "Regional geology and petroleum systems of the Illizi–Berkine area of the Algerian Saharan Platform: An overview." In: *Marine and Petroleum Geology* 27.1, pp. 143–178. ISSN: 02648172. DOI: 10.1016/j.marpetgeo.2008.10.002. URL: https://linkinghub.elsevier.com/retrieve/pii/S0264817209000464 (visited on 12/19/2019).

Gharsalli, Ramzi and Mourad Bédir (Dec. 2020). "Sequence stratigraphy of the subsurface cambro-ordovician siliciclastic deposits in the Chotts basin, Southern Tunisia: Petroleum implications." In: *Journal of African Earth Sciences* 172, p. 103997. ISSN: 1464343X. DOI: 10.1016/j.jafrearsci.2020.103997. URL: https://linkinghub.elsevier.com/retrieve/pii/S1464343X2030248X (visited on 10/03/2020).

Guiraud, R., W. Bosworth, J. Thierry, and A. Delplanque (Oct. 2005). "Phanerozoic geological evolution of Northern and Central Africa: An overview." In: *Journal of African Earth Sciences* 43.1, pp. 83–143. ISSN: 1464343X. DOI: 10.1016/j.jafrearsci.2005.07.017. URL: https://linkinghub.elsevier.com/retrieve/pii/S1464343X05001147 (visited on 12/19/2019).

Hantschel, Thomas and Armin Ingo Kauerauf (2009). *Fundamentals of Basin and Petroleum Systems Modeling*. Berlin, Heidelberg: Springer Berlin Heidelberg. ISBN: 978-3-540-72317-2 978-3-540-72318-9. DOI: 10.1007/978-3-540-72318-9. URL: http://link.springer.com/10.1007/978-3-540-72318-9 (visited on 04/15/2020).

Harris, Nicholas B. and Kenneth E. Peters, eds. (2012). *Analyzing the Thermal History of Sedimentary Basins: Methods and Case Studies*. SEPM (Society for Sedimentary Geology). ISBN: 978-1-56576-315-9 978-1-56576-317-3. DOI: 10.2110/sepmsp.103. URL: http://sp.sepmonline.org/content/sepspecpub/sepsp103/1.toccontent/103 (visited on 05/27/2020).

Jabir, A., A. Cerepi, C. Loisy, and J.-L. Rubino (Mar. 2020). "Stratigraphy, sedimentology and paleogeography of a Paleozoic succession, Ghadames and Jefarah basin, Libya and Tunisia." In: *Journal of African Earth Sciences* 163, p. 103642. ISSN: 1464343X. DOI: 10.1016/j.jafrearsci.2019.103642. URL: https://linkinghub.elsevier.com/retrieve/pii/S1464343X19302973 (visited on 03/17/2020).

Jarvie, Daniel M, Brenda Claxton, Bo Henk, John Breyer, Claxton Consulting, and Purple Martin (June 2001). "Oil and Shale Gas from Barnett Shale, Ft. Worth Basin, Texas." In: p. 29.

Lee, Eun Young, Johannes Novotny, and Michael Wagreich (2019). *Subsidence Analysis and Visualization*. SpringerBriefs in Petroleum Geoscience & Engineering. Cham: Springer International Publishing. ISBN: 978-3-319-76423-8 978-3-319-76424-5. DOI: 10.1007/978-3-319-76424-5. URL: http://link.springer.com/10.1007/978-3-319-76424-5 (visited on 04/15/2020).

Lüning, S. (2005). "AFRICA | North African Phanerozoic." In: *Encyclopedia of Geology*. Elsevier, pp. 12–25. ISBN: 978-0-12-369396-9. DOI: 10.1016/B0-12-369396-9/00472-X. URL: https://linkinghub.elsevier.com/retrieve/pii/B012369396900472X (visited on 03/17/2020).

Lüning, S, J Craig, D.K Loydell, P Štorch, and B Fitches (Mar. 2000). "Lower Silurian 'hot shales' in North Africa and Arabia: regional distribution and depositional model." In: *Earth-Science Reviews* 49.1, pp. 121–200. ISSN: 00128252. DOI: 10.1016/S0012-8252(99)00060-4. URL: https://linkinghub.elsevier.com/retrieve/pii/S0012825299000604 (visited on 05/06/2020).

Magoon, Leslie B. and Wallace G. Dow (1994). *The Petroleum System—From Source to Trap*. American Association of Petroleum Geologists. ISBN: 978-1-62981-092-8. DOI: 10.1306/M60585. URL: https://doi.org/10.1306/M60585.

Mann, U., T. Hantschel, R. G. Schaefer, B. Krooss, D. Leythaeuser, R. Littke, and R. F. Sachsenhofer (1997). "Petroleum Migration: Mechanisms, Pathways, Efficiencies and Numerical Simulations." In: *Petroleum and Basin Evolution*. Ed. by Dietrich H. Welte, Brian Horsfield, and Donald R. Baker. Berlin, Heidelberg: Springer Berlin Heidelberg, pp. 403–520. ISBN: 978-3-540-61128-8 978-3-642-60423-2. DOI: 10.1007/978-3-642-60423-2_8. URL: http://link.springer.com/10.1007/978-3-642-60423-2_8 (visited on 10/02/2020).

Mejri, Fathia, Pierre Félix Burollet, and Ali Ben Ferjani (2006). *Petroleum geology of Tunisia : a renewed synthesis*. Tunis: Enterprise tunisienne d'activités pétrolières.

Mohamed, Anis Belhaj, Ibrahim Bouazizi, and Moncef Saidi (Jan. 2014). "Oil-Oil Correlation and Potential Source Rocks in the Chotts Basin, Tunisia." In: *Proceedings of 7th International Petroleum Technology Conference*. 7th International Petroleum Technology Conference. Society of Petroleum Engineers. ISBN: 978-1-61399-235-7. DOI: 10.2523/17302-MS. URL: http://www.onepetro.org/mslib/servlet/onepetropreview?id=IPTC-17302-MS&soc=IPTC (visited on 09/09/2020).

Munz, Ingrid Anne (Jan. 2001). "Petroleum inclusions in sedimentary basins: systematics, analytical methods and applications." In: *Lithos* 55.1, pp. 195–212. ISSN: 00244937. DOI: 10.1016/S0024-4937(00)00045-1. URL: https://linkinghub.elsevier.com/retrieve/pii/S0024493700000451 (visited on 10/02/2020).

Peters, Kenneth E., Clifford C. Walters, and Paul J. Mankiewicz (Mar. 2006). "Evaluation of kinetic uncertainty in numerical models of petroleum generation." In: *AAPG Bulletin* 90.3, pp. 387–403. ISSN: 0149-1423. DOI: 10.1306/10140505122. URL: http://search.datapages.com/data/doi/10.1306/10140505122 (visited on 05/26/2020).

Peters, Kenneth and Mary Cassa (1994). "Applied Source Rock Geochemistry." In: *AAPG Memoir* 60.

Peyton, S. Lynn and Barbara Carrapa (Jan. 1, 2013). "An Introduction to Low-temperature Thermochronologic Techniques, Methodology, and Applications." In: *Application of Struc-*

tural Methods to Rocky Mountain Hydrocarbon Exploration and Development. Ed. by Constance N. Knight, Jerome J. Cuzella, and Leland D. Cress. Vol. 65. American Association of Petroleum Geologists, p. 0. ISBN: 978-0-89181-071-1. DOI: 10.1306/13381688St653578. URL: https://doi.org/10.1306/13381688St653578 (visited on 09/23/2020).

Raulin, Camille, Dominique Frizon de Lamotte, Samir Bouaziz, Sami Khomsi, Nicolas Mouchot, Geoffrey Ruiz, and François Guillocheau (Aug. 2011). "Late Triassic–early Jurassic block tilting along E–W faults, in southern Tunisia: New interpretation of the Tebaga of Medenine." In: *Journal of African Earth Sciences* 61.1, pp. 94–104. ISSN: 1464343X. DOI: 10.1016/j.jafrearsci.2011.05.007. URL: https://linkinghub.elsevier.com/retrieve/pii/S1464343X11001117 (visited on 12/19/2019).

Reiners, Peter W. and Mark T. Brandon (May 2006). "USING THERMOCHRONOLOGY TO UNDERSTAND OROGENIC EROSION." In: *Annual Review of Earth and Planetary Sciences* 34.1, pp. 419–466. ISSN: 0084-6597, 1545-4495. DOI: 10.1146/annurev.earth.34.031405.125202. URL: http://www.annualreviews.org/doi/10.1146/annurev.earth.34.031405.125202 (visited on 10/02/2020).

Selley, Richard C. and Stephen A. Sonnenberg (2015). *Elements of petroleum geology*. Third edition. Amsterdam ; Boston: Elsevier, Academic Press is an imprint of Elsevier. 507 pp. ISBN: 978-0-12-386031-6.

Smith, R.Y. (Nov. 2020). "Regional Geology and Fracture Network Characterisation of the Chotts and Jeffara Basins." MSc. Delft: Delft University of Technology.

Soua, Mohamed (Nov. 18, 2014a). "Early Carnian anoxic event as recorded in the southern Tethyan margin, Tunisia: an overview." In: *International Geology Review* 56.15, pp. 1884–1905. ISSN: 0020-6814, 1938-2839. DOI: 10.1080/00206814.2014.967315. URL: https://www.tandfonline.com/doi/full/10.1080/00206814.2014.967315 (visited on 03/17/2020).

– (Dec. 2014b). "Paleozoic oil/gas shale reservoirs in southern Tunisia: An overview." In: *Journal of African Earth Sciences* 100, pp. 450–492. ISSN: 1464343X. DOI: 10.1016/j.jafrearsci.2014.07.009. URL: https://linkinghub.elsevier.com/retrieve/pii/S1464343X14002271 (visited on 12/19/2019).

Sweeney, Jerry J. and Alan K. Burnham (Oct. 1990). "Sweeney et al (1990) Evaluation of a Simple Model of Vitrinite Reflecance Based on Chemical Kinetics.pdf." In: *The American Association of Petroleum Geologists Bulletin* 74.10, pp. 1559–1570.

Underdown, R., J. Redfern, and F. Lisker (Dec. 2007). "Constraining the burial history of the Ghadames Basin, North Africa: an integrated analysis using sonic velocities, vitrinite reflectance data and apatite fission track ages." In: *Basin Research* 19.4, pp. 557–578. ISSN: 0950-091X, 1365-2117. DOI: 10.1111/j.1365-2117.2007.00335.x. URL: http://doi.wiley.com/10.1111/j.1365-2117.2007.00335.x (visited on 03/17/2020).

Underdown, Ruth (2006). "AN INTEGRATED BASIN MODELLING STUDY OF THE GHADAMES BASIN, NORTH AFRICA." In: p. 609.

Underdown, Ruth and Jonathan Redfern (Jan. 2008). "Petroleum generation and migration in the Ghadames Basin, north Africa: A two-dimensional basin-modeling study." In: *AAPG Bulletin* 92.1, pp. 53–76. ISSN: 0149-1423. DOI: 10.1306/08130706032. URL: http://search.datapages.com/data/doi/10.1306/08130706032 (visited on 05/20/2020).

Voorn, Maarten, Ulrike Exner, Auke Barnhoorn, Patrick Baud, and Thierry Reuschlé (Mar. 2015). "Porosity, permeability and 3D fracture network characterisation of dolomite reservoir rock samples." In: *Journal of Petroleum Science and Engineering* 127, pp. 270–

285. ISSN: 09204105. DOI: 10.1016/j.petrol.2014.12.019. URL: https://linkinghub.elsevier.com/retrieve/pii/S0920410514004318 (visited on 01/26/2020).

Welte, Dietrich H, Brian Horsfield, and Donald R Baker (1997). *Petroleum and Basin Evolution Insights from Petroleum Geochemistry, Geology and Basin Modeling*. OCLC: 864578758. Berlin: Springer Berlin. ISBN: 978-3-642-64400-9.

Wust, Raphael A.J., Brent R. Nassichuk, Ron Brezovski, Paul C Hackley, and Nicole Willment (2013). "Vitrinite reflectance versus pyrolysis Tmax data: Assessing thermal maturity in shale plays with special reference to the Duvernay shale play of the Western Canadian Sedimentary Basin, Alberta, Canada." In: *SPE Unconventional Resources Conference and Exhibition-Asia Pacific*. SPE Unconventional Resources Conference and Exhibition-Asia Pacific. Brisbane, Australia: Society of Petroleum Engineers. DOI: 10.2118/167031-MS. URL: http://www.onepetro.org/doi/10.2118/167031-MS (visited on 05/06/2020).

Wygrala, B.P. (Oct. 1989). "Integrated Study of an Oil Field in the Southern Po Basin, Northern Italy." PhD thesis. Cologne, Germany: University of Cologne.

Yalçin, M. N., R. Littke, and R. F. Sachsenhofer (1997). "Thermal History of Sedimentary Basins." In: *Petroleum and Basin Evolution: Insights from Petroleum Geochemistry, Geology and Basin Modeling*. Ed. by Dietrich H. Welte, Brian Horsfield, and Donald R. Baker. Berlin, Heidelberg: Springer Berlin Heidelberg, pp. 71–167. ISBN: 978-3-642-60423-2. DOI: 10.1007/978-3-642-60423-2_3. URL: https://doi.org/10.1007/978-3-642-60423-2_3.

Zaafouri, Adel, Sofiene Haddad, and Beya Mannaî-Tayech (May 2017). "Subsurface Permian reef complexes of southern Tunisia: Shelf carbonate setting and paleogeographic implications." In: *Journal of African Earth Sciences* 129, pp. 944–959. ISSN: 1464343X. DOI: 10.1016/j.jafrearsci.2017.02.032. URL: https://linkinghub.elsevier.com/retrieve/pii/S1464343X17301000 (visited on 12/19/2019).

APPENDIX

a EXAMPLE STRATIGRAPHIC COLUMN AND LITHOLOGY

			Age [Ma]	Horizon	Depth [m]	Thick-ness [m]	Layer ID	Erosion Balance [m]		Lithology
								Max	Min	
1			1	Plio-Quaternary	0	142	PLIO_QUAT			Sandstone (typical)
15	Cenozoic		15	Miocene	142	0	TRANSGRESSION			Limestone (shaly)
66	Cretaceous	Upper Cretaceous	66	Senonian carbonates	142	458	SENONIAN CARBONATES			Dolomite (typical)
75			75	Senonian evaporates	600	341	SENONIAN EVAPORITES			Anhydrite
89			89	Zebbag Turonian	941	117	ZEBBAG TURONIAN			Dolomite (typical)
94			94	Zebbag Cenomanian	1058	192	ZEBBAG CENOMANIAN			Limestone (micrite)
100		Lower Cretaceous	100	Albian	1250	146	ALBIAN			Limestone (shaly)
113			113	Aptian	1396	79	APTIAN			Limestone (shaly)
126			126	Austrian phase	1475	0	AUSTRIAN	-955	-455	
130			130	Continental intercalaire	1475	345	LOWER CRETACEOUS	955	455	Sandstone (clay rich)
145	Jurassic	Malm	145	Sebaia	1820	339	SEBAIA			Dolomite (typical)
166			166	J1 Limestone	2159	218	J1			Dolomite (typical)
171		Dogger	171	Dogger	2377	339	DOGGER			Limestone (shaly)
183		Lias	183	Lias anhydrite	2716	280	LIAS ANHYDRITES			Anhydrite
190			190	Lias B Horizon	2996	25	B HORIZON			Dolomite (typical)
201	Triassic	Late	201	Triassic evaporates	3021	266	TRIASSIC EVAPORITES			Anhydrite
205			205	Triassic salt	3287	52	TRIASSIC SALT			Salt
209			209	D2	3339	35	D2 HORIZON			Dolomite (typical)
215			215	TAGS	3374	50	TAGS			Sandstone (clay rich)
228			228	Upper Volcanics 1	3424	19	VOLCANICS 2			Andesite (igneous)
235			235	Upper Volcanics 2	3443	47	VOLCANICS 1			Andesite (igneous)
237		Middle	237	TAGI	3490	39	TAGI			Sandstone (clay rich)
241			241	Triassic massive volcanic	3529	99	MASSIVE VOLCANICS			Andesite (igneous)
250	Permian		250	Hercynian phase 2	3628	0	HERCYNIAN 2	-1000	-400	
260			260	Permian	3628	0	PERMIAN	1000	400	Sandstone (clay rich)
290	Carboni-ferous		290	Hercynian phase 1	3628	0	HERCYNIAN 1	-2250	-950	
307			307	Carboniferous	3628	0	CARBONIFEROUS	700	400	Sandstone (typical)
370	Devonian		370	Devonian	3628	0	DEVONIAN	1200	500	Limestone (shaly)
410	Silurian		410	Fegaguira	3628	13	FEGAGUIRA	350	50	Shale (organic rich, typical)
419			419	Hot Shales	3641	38	HOT SHALES			Shale (organic rich, typical)
423			423	Jeffara equivalent	3678	0	JEFFARA			Sandstone (clay rich)
462	Ordovician		462	Azel	3678	3	AZEL			Shale (organic rich, typical)
476			476	Hamra	3681	62	HAMRA			Sandstone (typical)
478			478	El Atchane	3743	58	EL ATCHANE			Sandstone (typical)
483			483	El Gassi	3801	168	EL GASSI			Siltstone (organic rich, typical)

Figure a.1: Example of stratigraphic column and lithology used throughout the 1D and 2D back-stripping process.

b ADDITIONAL PROFILES MIGRATION STUDY

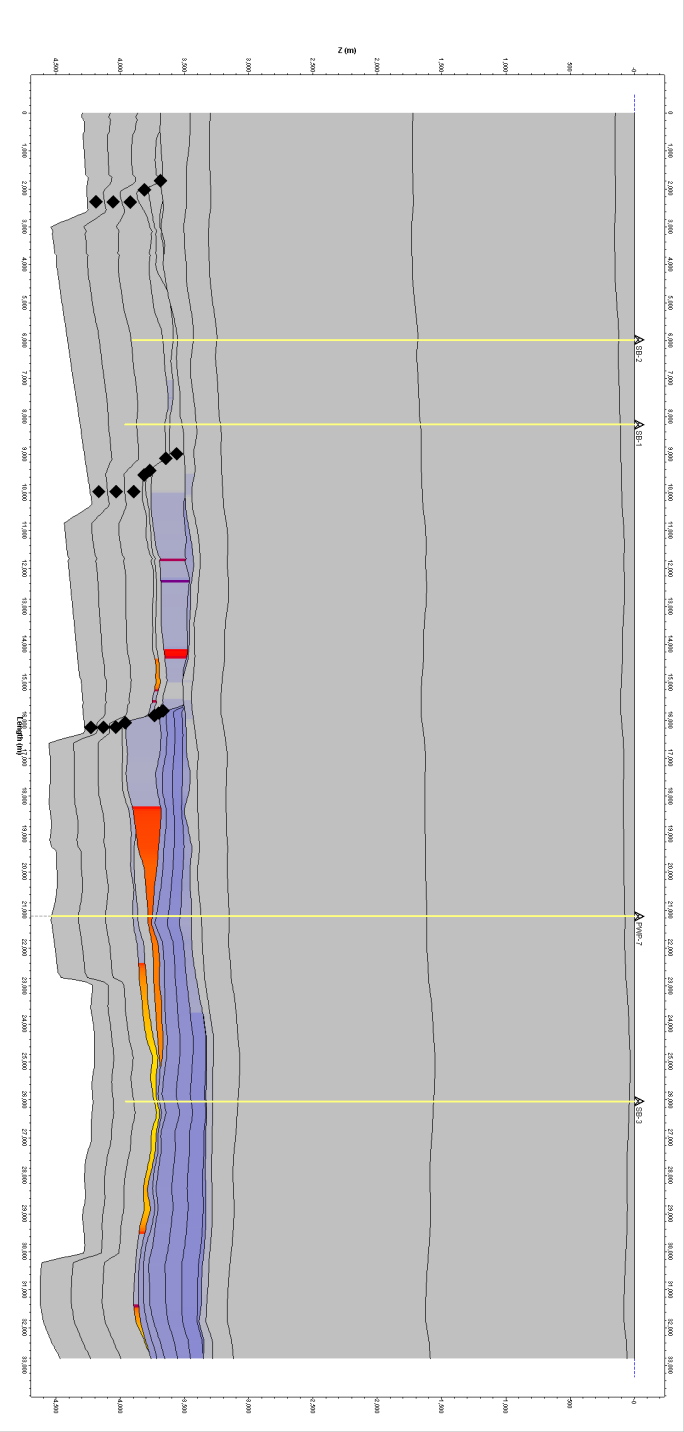

Figure b.1: Simulated hydrocarbon accumulations at present day along profile 7.

C PROPOSAL PERMEABILITY FIELD MEASUREMENTS

FIELD MISSION

Samples from the Permian deposits will have to be obtained during a field mission to the Medenine area, Central Tunisia (figure 2.1). This location was explored during a previous field mission, which helps with selecting measurement locations. The field mission is planned to last about 10 days in late March - early April as temperatures in the field will still be favorable.

Figure c.1: Angular unconformity outcropping in the Tebaga de Medenine (figure **??**). Mesozoic deposits are unconformably overlying Permian deposits.

The main objective of the field mission is to gather permeability measurements using the TinyPerm hand-held air permeameter. This device offers a permeability range of 1 mD −10 D for intact rock. Before departure I will test the TinyPerm on previously collected Permian- and Triassic samples, which will require coring, in the lab to determine whether their permeability lies within the TinyPerm's range. Depending on the results, we will select the main objective, with a preference for the Permian deposits.

To maximize the outcropping surface covered, TinyPerm measurements will be collected along transects perpendicular (roughly N-S) to the 2 major ridges in the Tebaga de Medenine (figure c.2). Measuring several transects along the ridges (E-W) captures

the large scale horizontal heterogeneity. Moving up vertically along the outcrop allows to characterise the vertical heterogeneity.

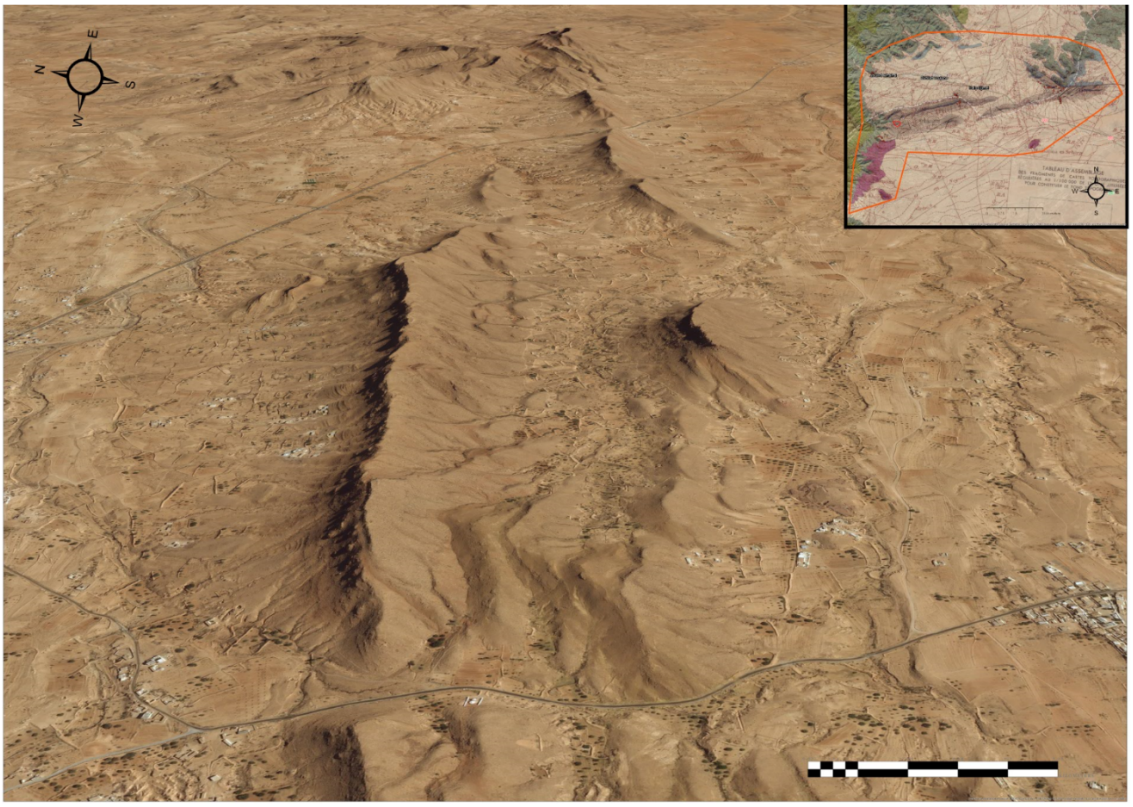

Figure c.2: Outcropping E-W ridges containing Permian packages in the Tebaga de Medenine. TinyPerm measurements will be collected perpendicular to these ridges. Figure **??** shows the precise location of the Tebaga de Medenine.

Measuring on cleared outcropping surfaces with systematic spacing is beneficial for transferring to a numerical grid for up-scaling purposes. Measurement spacing depends on layer geometry and required time for measurements. Measurement locations are tracked using GPS, photo's and logs in both horizontal- and vertical direction.

TinyPerm measurements will be processed during the field mission to capture the permeability range per facies and measurement location. This allows us to sample effectively, aiming to take outcrop samples representing the facies permeability range. Lab experiments will result in a more reliable correlation with the TinyPerm measurements using this approach.

To quantify the degree of compaction the outcrop samples have undergone, we will carefully investigate the macro-scale structures in the field i. e. bedding and stylolites. This will be helpful for the sample's burial depth estimations and evaluate whether the sample is useful for laboratory experiments.

To investigate difference between lithofacies a description of the Permian sandstone and -carbonates will be constructed in the field. We will attempt to determine relative thicknesses and orientation trends and use this information in the 3D subsurface model. Both lithofacies will be characterised using TinyPerm measurements such that they can be implemented separately in the 3D subsurface model.

In addition, we will be analysing the regional geological structure in the Medenine area to better understand the evolution of the basin through time. The Tebaga de Medenine hosts the only outcropping Permian deposits in Tunisia and shows Mesozoic deposits unconformably overlying Permian deposits (figure c.1). It provides a perfect opportunity to gather bedding measurements to characterise the geometry of the unconformity.

Apart from the Tebaga de Medenine, there are other locations that could prove helpful in our objectives. Figure c.3 shows two additional locations in the Medenine area that could improve our understanding of the timing of deformation in the Southern Chotts Basin. East of the Tebaga the Koutine area hosts an outcrop which possibly contains more Permian deposits. South of the Tebaga, near Bharya, Triassic deposits crop out and allow for further characterise the geometry of the Mesozoic package deposited after the orogenic event.

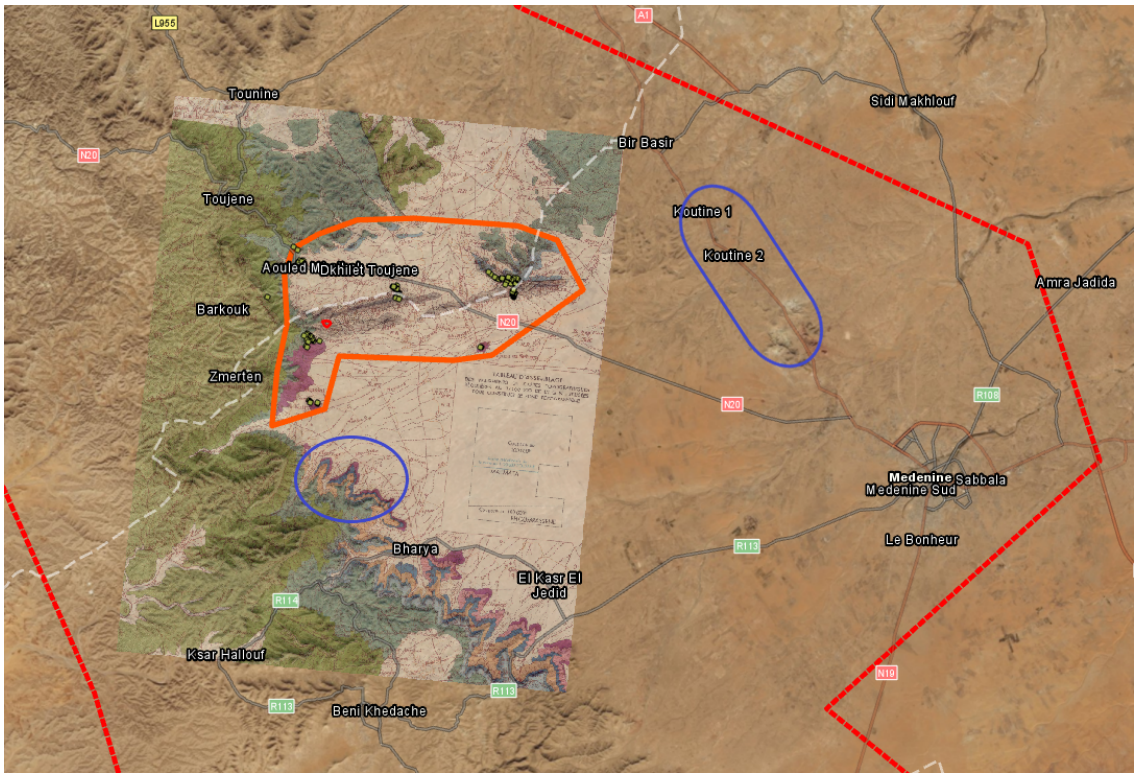

Figure c.3: Two additional locations south and east of the Tebaga de Medenine that could prove useful to understand the timing of deformation.

THIN SECTION ANALYSIS

Before using outcrop permeability to populate subsurface strata, differences in burial history and diagenesis must be quantified (Dutton and Willis, 1998). With help of the university of Utrecht, we will construct thin sections from the collected outcrop samples. Using polarisation microscopes, analysis of the thin sections' diagenetic features (i. e. pressure dissolution, compaction, fracturing, etc.) is possible. Addition of 'Alizarin Red S' distinguishes dolomite- and calcite crystals allows to quantify the degree of dolomitisation,

which may effect reservoir quality due to associated porosity and permeability changes (Ehrenberg et al., 2006).

The aim is to construct $30 - 40$ thin sections to capture the diagenetic heterogeneity of the samples. Investigation of the present diagenetic features helps us to estimate the degree of compaction. In combination with macro-scale observations in the field, thin section analysis allows us to estimate the samples' burial history. Comparing this with subsurface conditions indicates whether the outcrop samples have undergone similar compaction history and diagenesis. The outcome of the thin section analysis is the decisive factor for the laboratory approach.

LAB EXPERIMENTS

Lab experiments performed under increasing confining pressure show that permeability decreases significantly with increasing depth (Voorn et al., 2015). Therefore, field measurements gathered using the TinyPerm permeameter cannot be used directly as permeability input for a subsurface model. A relation between TinyPerm field measurements and their subsurface equivalent will be computed with lab experiments on samples extracted during the field mission. These samples represent the permeability ranges measured in the field for each formation and lithofacies.

Circa 30 samples obtained during the field mission require coring and preparation for the lab experiments. Liquid permeability measurements will be conducted under surface conditions (atmospheric pressure) with a constant head test. This results in a relation between the air permeability field measurements and the water permeability lab experiments.

Depending on the results of macro-scale field observations and thin section analysis there are two scenarios:

1. Outcrop samples are judged to have undergone similar diagenesis as subsurface rock and are estimated to be buried to similar depths. We select 3 samples for TerraTek experiments, which are time consuming and expensive. TerraTek experiments allow us to measure the liquid permeability under increasing confining pressure. The maximum confining pressure reached in TerraTek experiments is 50 MPa which translates to circa 1800 m depth, depending on the bulk density of the overburden. This will allow us to fit a relation to the sample's liquid permeability and confining pressure.

   Combining the relation between field- and lab measurements under surface conditions with the permeability-confining pressure relation allows us to convert TinyPerm measurements to subsurface equivalents.

2. Outcrop samples show a different diagenetic history and have been buried to different depths. Therefore, the collected samples are not directly representative for the subsurface strata. Results from the lab experiments under surface conditions will be compared with proven literature relations to obtain reasonable subsurface equivalents.

Numerical up-scaling requires the realistic subsurface equivalents provided by one of the scenarios as input. Using this approach the $3D$ subsurface model can be populated with realistic permeability data obtained through field measurements.